Film growth viewed as stochastic dot processes

2005 J. Phys.: Condens. Matter 17 R571

(http://iopscience.iop.org/0953-8984/17/17/R02)

INSTITUTE OF PHYSICS PUBLISHING JOURNAL OF PHYSICS: CONDENSED MATTER

J. Phys.: Condens. Matter **17** (2005) R571–R605 doi:10.1088/0953-8984/17/17/R02

TOPICAL REVIEW

Film growth viewed as stochastic dot processes

M Fanfoni[1] **and M Tomellini**[1,2]

[1] Dipartimento di Fisica, Università di Roma Tor Vergata, Via della Ricerca Scientifica 00133, Roma, Italy
[2] Dipartimento di Scienze e Tecnologie, Chimiche Università di Roma Tor Vergata, Via della Ricerca Scientifica 00133, Roma, Italy

Received 9 November 2004, in final form 20 January 2005
Published 15 April 2005
Online at stacks.iop.org/JPhysCM/17/R571

Abstract

In this article some results regarding film growth considered as a stochastic process of dots are reviewed. The central concept of the theory described in the initial part of the article is the evaluation of the exclusion probability, i.e. the probability that no dots are found in a given region of the surface. This is reviewed to a certain extent for both correlated and uncorrelated dots and, moreover, for distinguishable classes of dots. This theoretical framework allows one to tackle the nucleation and growth of films ruled by diffusion of adspecies. In this specific instance the theory has been employed for computing the coverage dependent characteristic times for monomer capture from islands and for island collision, in the case of impingement and/or coalescence mechanisms. The ultimate aim is to model, by means of rate equations, the kinetics of film formation over the whole range of coverage.

Contents

1. Introduction

Thin film growth and, more generally, random growth are worth studying in themselves. In fact, they are related to a lot of interesting subjects of applied mathematics, for instance the fascinating world of stochastic processes. Moreover, film growth embodies several intriguing concepts such as self-similarity, self-affinity, universality class, Voronoi tessellation, scaling chaos, as well as the interesting physical question of which roughening, growth instabilities, local growth, spatial correlation, Ostwald ripening are just a few examples [1]. Moreover, film growth is also of great importance in several areas of technology, which range from surface coatings to catalysts, from heterojunctions to nanostructure fabrication for electronic devices, which have been winning considerable attention during the last few years. Several film growth methods have already been developed in which the deposition occurs from both liquid and vapour phases. As regards the deposition from the liquid phase, in addition to liquid phase epitaxy (LPE), it is worth mentioning electrochemical film formation (EFF) which consists in nucleation and crystal growth in electrochemical systems under the influence of an electric field [2]. As far as the depositions from vapour phases are concerned, two large classes of techniques have been worked out, namely chemical vapour deposition (CVD) and physical vapour deposition (PVD). The former is the most common thin film deposition method, especially in advanced semiconductor manufacturing. The new phase is formed as a result of chemical reaction between gaseous reactants, usually at high temperatures, close to the substrate. The product of the reaction deposits itself on the surface. This method is used to deposit films of semiconductors (crystalline and non-crystalline) and insulators, as well as metals. In PVD the material is physically transferred, in the vacuum environment, from the source to the substrate without involving any chemical reaction. This process can be carried out by means of thermal and/or electron beam heating or mechanically removing atoms from the source through ion sputtering [3].

In this article we will deal with thin film formation characterized by nucleation and growth where nucleation of adspecies at the surface strongly affects the kinetics of growth. These conditions are encountered whenever a concentration of adspecies and, in turn, a diffusion process are established on the substrate as, for example, in PVD and EFF.

Some specifications of notation are in order for the sake of clarity. Basically three terms will be freely used throughout the article: cluster, island and nucleus. The first is an aggregate of atoms related to a single nucleation event, the second is an isolated object made up, in general, of connected clusters; 'nucleus' stands for the smallest stable cluster.

As a matter of fact the diffusion process has a tremendous impact on the film morphology. In fact, as regards this aspect, there are at least three effects that must be taken into account. In the first place, because of the adatom diffusion towards stable islands, *a zone around each island is established where the nucleation rate is reduced* [4]. The reason is basically that the closer the adspecies is to an island, the larger the probability of capture. The second effect follows from the fact that the growth of each island is linked to the related Voronoi cell (VC) [5–7], or, more properly, 'edge cells' [8]. Incidentally, this implies that, even in the simultaneous nucleation case and before cluster impingement, the film morphology is characterized by a distribution of island sizes. In the third place, during the island growth, nucleation is still possible within the Voronoi cell, the extension of the diffusion zone (see the first effect) being, in relation to the distances among the island borders, the crucial parameter for nucleation. These issues are so important from the conceptual point of view that it is worth illustrating them graphically. In figure 1 we show a circular island in its Voronoi cell at two different times. The dashed circles represent the region where nucleation is almost forbidden. In the following this region will be referred to as the nucleation forbidden zone (NFZ) [9].

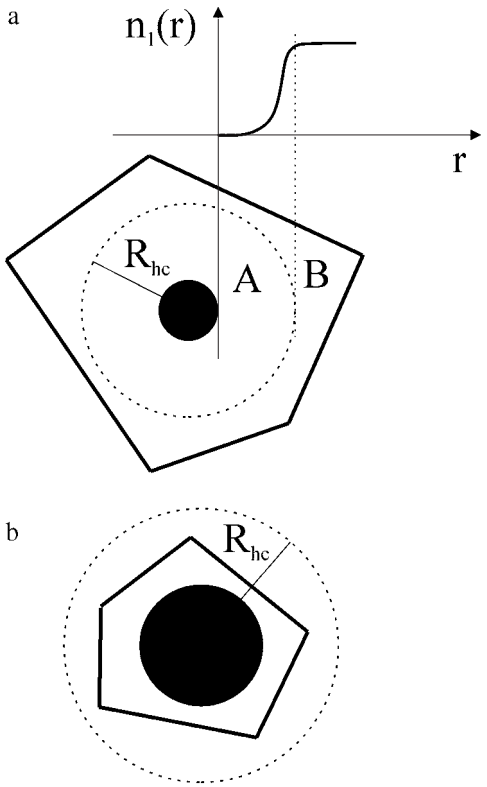

Figure 1. Pictorial view of a circular island in its Voronoi cell, at two values of the growth time: t_1 (panel (a)) and $t_2 > t_1$ (panel (b)). Around each island there exists a region in which nucleation is nearly forbidden, because of admonomer depletion caused by island growth. This is the circular region A displayed in panel (a). The concentration profile of the adatoms in the Voronoi cell is also displayed. During the island growth the NFZ can exceed the size of the Voronoi cell and, as a consequence, island growth is the only process occurring in the VC (panel (b)). Islands are spatially correlated within the R_{hc} length.

In panel (a) a sketch of the concentration profile of adatoms close to the island is also shown, as expected from the nature of the process (diffusion). In addition, two generic points inside the VC, namely A and B, respectively inside and outside the NFZ, are displayed[3]. The probability of nucleation is proportional to the adatom population and, by reason of the concentration profile, the probability of nucleation in B is larger than that in A. Moreover, on assuming that adatoms do not 'escape' from the VC, the probability that an adatom be captured by the island in A is larger than that for B. On the other hand, when the NFZ becomes larger than the VC, the nucleation probability drops to zero and, consequently, the island growth is the only allowed process.

It is apparent that in such a situation nuclei and islands are spatially correlated. In particular, at least two phenomena can be envisaged. Firstly, because of the NFZ, the nucleation does not take place over the whole available space; thus a non-Poissonian space distribution of nuclei comes about. Secondly, the growth of each nucleus depends upon the size of its VC which, in turn, is a time dependent quantity. As a consequence, a local growth law is established which gives rise to correlation effects among islands. In other words there is not

[3] For the sake of simplicity, in this article the forbidden zone is modelled through the Heaviside function.

a unique growth law for all nuclei. However, depending on the stochastic approach which is employed, it is possible to resort to an average growth law. This allows one to extend the analytical approach with respect to the numerical one.

Experimentally, the spatially correlated nucleation has been detected, for example, by Yang *et al* [10] and by Cherepanov *et al* [11], the former studying the nucleation of Ge on GaAs at 695 K, the latter studying Si and Ge nucleation on Si(111) with Bi as a surfactant.

Another phenomenon which has to be considered in thin film formation is the coalescence or impingement of islands. Also in this case a clarification of the terminology is mandatory. In the case of coalescence the distribution of matter among islands occurs under conservation of both mass and island shape and, as far as three-dimensional islands are concerned, by a reduction of the surface coverage too. In contrast, in the impingement case no redistribution of matter takes place after collisions among islands [12] and each cluster retains its individuality. Confining the analysis to the Poissonian nucleation, the kinetics of the number of islands can be modelled analytically in film growth ruled by both impingement and coalescence processes. Surprisingly, for the simultaneous nucleation case, the same behaviour of the island density, as a function of surface fraction coverage, is obtained for both mechanisms.

In order to describe the kinetics of thin film growth, several methods have been developed, which include kinetic Monte Carlo [13], stochastic differential equations [14] and rate equations [1, 15] approaches. As we are interested in the time evolution of the fraction of substrate surface covered by islands and in the number of islands, remaining in a semianalytical framework, the rate equation approach is certainly the most suitable. From the historical point of view, rate equations have been adopted for investigating the early stage of thin film growth, from the beginning to the nucleation regime or just beyond it. On the other hand, to study the kinetics over the entire range of surface coverage, it is necessary to take into account the aforementioned phenomenon of island collision that, as a kinetic process, can be modelled, after all, using a suitable time constant. In addition, also the time constant related to the growth has to be modelled over the whole range of surface coverage. This quantity is nothing but the lifetime of the monomer that performs a random walk on the surface before being captured by an island. The two time constants depend upon the coverage and their knowledge allows one to solve rate equations over the full range of coverage. Last but not least is the possibility of treating, in the framework of a rate equation approach, even a non-random nucleation process [16].

The present article is organized as follows. In the next section the theoretical background, which rests on probability theory, is reviewed. The results stemming from the stochastic treatment directly lead to the computation of the fractional surface coverage, the adatom lifetime and the collision series, as we will show in section 3. They are all basic ingredients for modelling, by means of a rate equation, thin film growth. To this topic section 4 is devoted.

2. Theoretical background

In this section the theoretical background is outlined, the results of which will be employed in the next section. In particular, in this section we determine the exclusion probability, that is the probability that, given a distribution of dots in a two-dimensional (2D) space, no one of them falls in a given finite region. On the grounds of this probability we will see how it is possible to derive a set of kinetic quantities for describing the film growth.

2.1. Formulation for a single class of dots

The basic question to answer is rather simple to state: *given a distribution of dots in a 2D space, what is the probability of finding a 2D region, let us say* Δ, *empty of dots?* Otherwise,

what is the probability that a plane figure, Δ*, could be accommodated in a space not including any dot?*

In order to answer this question, we will make use of the correlation function formalism which is described to a certain extent in the excellent textbook by Van Kampen [17] from which we will borrow notation and follow.

To begin with, let us introduce the sample space. Each element (or state) of the space consists of: (i) a non-negative number s; (ii) for each s, a set of 2D variables $\{\mathbf{x}_1, \ldots, \mathbf{x}_s\}$ each of them ranging over the entire space.

The probability density function over these states is given by a sequence of non-negative functions $Q_s(\mathbf{x}_1, \ldots, \mathbf{x}_s)$, which obey the normalization condition

$$Q_0 + \sum_{s=1}^{\infty} \frac{1}{s!} \int \mathrm{d}\mathbf{x}_1 \ldots \mathrm{d}\mathbf{x}_s \, Q_s(\mathbf{x}_1, \ldots, \mathbf{x}_s) = 1, \tag{1}$$

where the presence of the factorial is due to the fact that the $s!$ sets $\{\mathbf{x}_1, \ldots \mathbf{x}_s\}$ are indistinguishable. In addition, the Q_s s are symmetric functions of their variables.

The function 'number of dots in the domain Δ', N, defined in the same sample space as the Q_s s, can be written by introducing the indicator $\chi(\mathbf{x})$ in such a way that $\chi(\mathbf{x}) = 1$ for $\mathbf{x} \in \Delta$ and $\chi(\mathbf{x}) = 0$ otherwise. Thus N is represented by the sequence $\{0, N_1(\mathbf{x}_1), N_2(\mathbf{x}_1, \mathbf{x}_2), \ldots, N_s(\mathbf{x}_1, \ldots, \mathbf{x}_s)\}$ where

$$N_s(\mathbf{x}_1, \ldots \mathbf{x}_s) = \sum_{k=1}^{s} \chi(\mathbf{x}_k). \tag{2}$$

Following the calculation reported in appendix A, the mean value of N and N^2 can be written as follows:

$$\langle N \rangle = \int_{\Delta} \mathrm{d}\mathbf{x}_1 \, f_1(\mathbf{x}_1) \tag{3}$$

$$\left\langle N^2 \right\rangle = \langle N \rangle + \int_{\Delta} \mathrm{d}\mathbf{x}_1 \int_{\Delta} \mathrm{d}\mathbf{x}_2 \, f_2(\mathbf{x}_1, \mathbf{x}_2), \tag{4}$$

where

$$f_n(\mathbf{y}_1, \ldots, \mathbf{y}_n) = \sum_{s=n}^{\infty} \frac{1}{(s-n)!} \int \mathrm{d}\mathbf{x}^{s-n} \, Q_s(\mathbf{y}_1, \mathbf{y}_2, \ldots, \mathbf{y}_n, \mathbf{x}_{n+1} \ldots, \mathbf{x}_s). \tag{5}$$

The functions $\{f_n\}$ will be referred to as f-functions; they are non-negative and symmetric in their arguments $\{\mathbf{x}_n\}$.

Let us consider now a generic function defined by the sequence

$$\begin{aligned} V &\equiv \{0, V_1(\mathbf{x}_1), V_2(\mathbf{x}_1, \mathbf{x}_2), \ldots, V_s(\mathbf{x}_1, \ldots, \mathbf{x}_s), \ldots\} \\ &= \left\{0, v_1(\mathbf{x}_1), \sum_{k=1}^{2} v_k(\mathbf{x}_k), \ldots, \sum_{k=1}^{s} v_k(\mathbf{x}_k) \ldots\right\} \end{aligned} \tag{6}$$

and the functional defined as

$$L[v] \equiv \left\langle \prod_{\sigma=1}^{s} \{1 + v(\mathbf{x}_\sigma)\} \right\rangle. \tag{7}$$

The following mean values are evaluated in appendix B:

$$\langle V \rangle = \int \mathrm{d}\mathbf{x}_1 \, v(\mathbf{x}_1) f_1(\mathbf{x}_1), \tag{8}$$

$$\left\langle V^2 \right\rangle = \int \mathrm{d}\mathbf{x}_1 \, v^2(\mathbf{x}_1) f_1(\mathbf{x}_1) + \int \mathrm{d}\mathbf{x}_1 \, \mathrm{d}\mathbf{x}_2 \, v(\mathbf{x}_1) v(\mathbf{x}_2) f_2(\mathbf{x}_1, \mathbf{x}_2). \tag{9}$$

In order to simplify the notation the set of all coordinates will be indicated by $\langle 1\rangle$, the set of all distinct couples of coordinates by $\langle 2\rangle$ and so on. By applying the term 'distinct' it is understood that, for example, the term $\mathbf{x}_\nu\mathbf{x}_\mu\mathbf{x}_\nu$ is the same as $\mathbf{x}_\nu\mathbf{x}_\nu\mathbf{x}_\mu$. Thus

$$\langle V\rangle = \left\langle \sum_{\langle 1\rangle} v \right\rangle = (vf_1) \tag{10}$$

$$\langle V^2\rangle = \left\langle \sum_{\langle 1\rangle} v \sum_{\langle 1\rangle} v \right\rangle = \left\langle \sum_{\langle 1\rangle} v^2 \right\rangle + 2\left\langle \sum_{\langle 2\rangle} vv \right\rangle = \left(v^2 f_1\right) + (vvf_2)\,, \tag{11}$$

where

$$(vf_1) \equiv \int \mathrm{d}\mathbf{x}_1\, v(\mathbf{x}_1) f_1(\mathbf{x}_1)$$

and

$$(vvf_2) \equiv \int \mathrm{d}\mathbf{x}_1\, \mathrm{d}\mathbf{x}_2\, v(\mathbf{x}_1)v(\mathbf{x}_2) f_2(\mathbf{x}_1, \mathbf{x}_2).$$

By the same method, the third moment becomes

$$\begin{aligned}\langle V^3\rangle &= \left\langle \sum_{\langle 1\rangle} v \sum_{\langle 1\rangle} v \sum_{\langle 1\rangle} v \right\rangle = \left\langle \sum_{\langle 1\rangle} v^3 + 3\sum_{\langle 2\rangle} v^2 v + 3!\sum_{\langle 3\rangle} vvv \right\rangle \\ &= (v^3 f_1) + 3(v^2 v f_2) + (vvvf_3).\end{aligned} \tag{12}$$

Equation (7) can be recast as

$$L[v] = \left\langle 1 + \sum_{\langle 1\rangle} v + \sum_{\langle 2\rangle} vv + \sum_{\langle 3\rangle} vvv + \cdots \right\rangle \tag{13}$$

and thanks to (10)–(12) this reads

$$L[v] = 1 + (vf_1) + \frac{1}{2}(vvf_2) + \frac{1}{3!}(vvvf_3) + \cdots = 1 + \sum_{n=1}^{\infty} \frac{1}{n!}(\{v\ldots v\}_n f_n), \tag{14}$$

where $\{v\ldots v\}_n \equiv v(\mathbf{x}_1)v(\mathbf{x}_2)\ldots v(\mathbf{x}_n)$. From equation (14) it follows that

$$\left(\frac{\delta^n L}{\delta v^n}\right)_{v=0} = f_n. \tag{15}$$

All these results allow one to evaluate, for instance, the characteristic function of the number N of dots in a given domain Δ defined by (2). In fact, if $v = \mathrm{e}^{\mathrm{i}k\chi} - 1$, from equations (7) and (14), we obtain

$$\left\langle \prod_{\langle 1\rangle} \mathrm{e}^{\mathrm{i}k\chi} \right\rangle = \left\langle \exp\left(\mathrm{i}k \sum_{\langle 1\rangle} \chi\right) \right\rangle = 1 + \sum_{n=1}^{\infty} \frac{1}{n!}\left(\mathrm{e}^{\mathrm{i}k} - 1\right)^n \int_\Delta f_n\, \mathrm{d}\mathbf{x}^n = \left\langle \mathrm{e}^{\mathrm{i}kN}\right\rangle, \tag{16}$$

from which, thanks to the general properties of the characteristic function, the probability P_E, from now on referred to as the *exclusion probability*, that no dots occur in the domain Δ is obtained as

$$P_E(\Delta) = 1 + \sum_{n=1}^{\infty} \frac{(-)^n}{n!} \int_\Delta f_n\, \mathrm{d}\mathbf{x}^n = L[-\chi]. \tag{17}$$

Equation (17) is the answer to our question. Nevertheless, it would be preferable and convenient to express the functional $L[v]$ through a cumulant expansion. To this end equation (14) becomes

$$L[v] = \exp\left(\sum_{n=1}^{\infty} \frac{1}{n!}(\{v\ldots v\}_n g_n)\right) \tag{18}$$

and, applying equation (15), it is not a difficult job to show that, in order for equation (18) to be true, the following cluster expansion must hold:

$$
\begin{aligned}
f_1(\mathbf{x}_1) &= g_1(\mathbf{x}_1)\\
f_2(\mathbf{x}_1,\mathbf{x}_2) &= g_1(\mathbf{x}_1)g_1(\mathbf{x}_1) + g_2(\mathbf{x}_1,\mathbf{x}_2)\\
f_3(\mathbf{x}_1,\mathbf{x}_2,\mathbf{x}_3) &= g_1(\mathbf{x}_1)g_1(\mathbf{x}_2)g_1(\mathbf{x}_3) + g_1(\mathbf{x}_1)g_2(\mathbf{x}_2,\mathbf{x}_3)\\
&\quad + g_1(\mathbf{x}_2)g_2(\mathbf{x}_1,\mathbf{x}_3) + g_1(\mathbf{x}_3)g_2(\mathbf{x}_1,\mathbf{x}_2) + g_3(\mathbf{x}_1,\mathbf{x}_2,\mathbf{x}_3).
\end{aligned}
\tag{19}
$$

For the special case $v = \mathrm{e}^{\mathrm{i}k\chi} - 1$, thanks to equation (18), we calculate

$$
\left\langle \mathrm{e}^{\mathrm{i}kN} \right\rangle = \exp\left(\sum_{n=1}^{\infty} \frac{1}{n!} \left(\mathrm{e}^{\mathrm{i}k} - 1\right)^n \int_{\Delta} g_n \, \mathrm{d}\mathbf{x}^n \right) \tag{20}
$$

and consequently the exclusion probability of having no dots in Δ reads

$$
P_E(\Delta) = \exp\left(\sum_{n=1}^{\infty} \frac{(-)^n}{n!} \int_{\Delta} g_n \, \mathrm{d}\mathbf{x}^n \right). \tag{21}
$$

2.2. Formulation for many classes of dots

The theory outlined in the previous sections concerns dots of the same kind, i.e. they all belong to the same class and are indistinguishable. The issue we want to deal with in the following is more involved: *we wish to compute P_E for a countable set of distinguishable classes of dots*. They are indistinguishable within each class and correlated with one another independently of the class to which they belong.

Each element (or state) of the sample space consists of: (i) a non-negative integer m; (ii) a non-negative integer s; (iii) an m-tuple of strictly positive integers $n_1 \ldots n_m$ such that $\sum_{\nu=1}^{m} n_\nu = s$; (iv) for each m, s and $(n_1 \ldots n_m)$, s 2D real variables exist, each of them ranging over the whole space:

$$
\underbrace{\{\mathbf{x}_1, \ldots, \mathbf{x}_{n_1}\}_1, \ldots, \{\mathbf{x}_1, \ldots, \mathbf{x}_{n_m}\}_m}_{s} \in \Re^{2s}.
$$

The probability density function over these states is given by a sequence of non-negative functions Q which obey the normalization condition

$$
Q^{(0)} + \sum_{\{1\}} \sum_{s} \sum_{\Pi^s_{\{1\}}} \frac{1}{n_i!} \int Q^{(1)}_{\pi^s_i} \, \mathrm{d}\mathbf{x}^s + \sum_{\{2\}} \sum_{s} \sum_{\Pi^s_{\{2\}}} \frac{1}{n_i!\, n_j!} \int Q^{(2)}_{\pi^s_{ij}} \, \mathrm{d}\mathbf{x}^s + \cdots = 1, \tag{22}
$$

where $\{n\}$ indicates the set of all distinct n-tuples of m classes. s is the total number of dots, m is the number of classes; thus necessarily $s \geqslant m$. $\Pi^s_{\{m\}}$ is the set which includes all partitions of s with m integers and their distinct permutations. For instance

$$
\Pi^5_{\{3\}} = \{(113), (131), (311), (122), (212), (221)\}.
$$

$\pi^s_{i_1 \ldots i_m}$ is an element of $\Pi^s_{\{m\}}$.

Let V be a function over the same state space as for the Q s of the form $V = V^{(1)} + V^{(2)} + \cdots$, where $V^{(m)} = \sum_{\{1\}}^{m} \sum_{\langle 1 \rangle}^{s} v_i(\mathbf{x}_v)$ and the subscript of v refers to the classes while that of $\mathbf{x}$ refers to the coordinates; then

$$
\langle V \rangle = \left\langle V^{(1)} \right\rangle_{\{1\}} + \left\langle V^{(2)} \right\rangle_{\{2\}} + \cdots \tag{23}
$$

$$
\left\langle V^k \right\rangle = \left\langle V^{(1)k} \right\rangle_{\{1\}} + \left\langle V^{(2)k} \right\rangle_{\{2\}} + \cdots. \tag{24}
$$

Here only the computation of $\langle V\rangle$ will be described in some detail (see appendix C); as far as the evaluation of $\langle V^2\rangle$ and $\langle V^3\rangle$ is concerned, the reader may consult [18]. The expressions read

$$\langle V\rangle = \sum_{\{1\}}(v_i f_i) \tag{25}$$

and

$$\left\langle V^2\right\rangle = \sum_{\{1\}}(v_i^2 f_i) + \sum_{\{1\}}\sum_{\{1\}}(v_i v_j f_{ij}), \tag{26}$$

where f_i and f_{ij} are the generalizations of equation (5) to the many-classes case (see appendix C).

Also in this case one can introduce a functional the derivatives of which with respect to $\{v_i\}$ provide the f-functions; it is

$$L[\{v\}] = \left\langle \prod_{\langle 1\rangle}^{n_i}\{1+v_i\}\prod_{\langle 1\rangle}^{n_j}\left\{1+v_j\right\}\ldots\right\rangle. \tag{27}$$

Exploiting the averages $\langle V^n\rangle$, equation (27) can be written as

$$L[\{v\}] = 1 + \sum_m \sum_{\{m\}}\sum_s\sum_{\Pi^s_{\{m\}}}\frac{1}{n_1!\ldots n_m!}(v_1^{n_1}\ldots v_m^{n_m} f_s\,(n_1\ldots n_m)),$$

$f_s(n_1\ldots n_m)$ being the f-function depending upon $s=\sum_{i=1}^m n_i$ variables of which n_1 are of class 1, n_2 of class 2 and so on. As in the single-class case, the f-functions are given by

$$\left(\frac{\delta^p L}{\delta^{p_1}v_1\delta^{p_2}v_2\ldots\delta^{p_k}v_k}\right)_{\{v\}=0} = f_p(p_1\ldots p_m), \tag{28}$$

where $p=\sum_{i=1}^m p_i$. The cumulant expansion reads

$$L[\{v\}] = \exp\left[\sum_m\sum_{\{m\}}\sum_s\sum_{\Pi^s_{\{m\}}}\frac{1}{n_1!\ldots n_m!}(v_1^{n_1}\ldots v_m^{n_m} g_s\,(n_1\ldots n_m))\right] \tag{29}$$

and, thanks to equation (28), it is possible to link f s to g s. At long last, the probability that no dots of the class i be in the Δ_i domain, no dots of class j be in the Δ_j domain etc can be evaluated and they read [18, 19]

$$P_E\,(\{\Delta\}) = \exp\left[\sum_m\sum_{\{m\}}\sum_s\sum_{\Pi^s_{\{m\}}}\frac{(-)^s\int_{\Delta_1}\mathrm{d}\mathbf{x}_1^{n_1^s}\ldots\int_{\Delta_m}\mathrm{d}\mathbf{x}_m^{n_m^s}\,g_s\,(n_1\ldots n_m)}{n_1!\ldots n_m!}\right]. \tag{30}$$

This last equation can be recast, as demonstrated in appendix D, as

$$P_E(\{\Delta\}) = \exp\left[\sum_s\frac{(-)^s}{s!}\sum_{i_1}\ldots\sum_{i_s}\rho_{i_1}\ldots\rho_{i_s}\int_{\Delta_{i_1}}\mathrm{d}\mathbf{x}^{(i_1)}\ldots\int_{\Delta_{i_s}}\mathrm{d}\mathbf{x}^{(i_s)}\,\tilde{g}_s(\mathbf{x}^{(i_1)}\ldots\mathbf{x}^{(i_s)})\right], \tag{31}$$

where

$$g_s \equiv \rho_1^{n_1}\ldots\rho_m^{n_m}\tilde{g}_s, \tag{32}$$

$\rho_1\ldots\rho_m$ being the densities of dots of classes $1,\ldots,m$, respectively. The i_k s run, independently, over all classes.

For the purpose of studying the film growth it is useful to transform equation (31) by considering a continuous distribution of classes of dots and this is readily achieved by

introducing a parameter t, such that $\mathrm{d}\rho = \frac{\mathrm{d}\rho}{\mathrm{d}t}\,\mathrm{d}t$, the sums over a countable set of classes, become integrals over the domain of t. It goes without saying that the domains of the arguments, as well as the arguments of g_s, also depend upon the parameter t. The exclusion probability reads

$$P_E(\{\Delta\}) = \exp\left[\sum_s \frac{(-)^s}{s!}\int \frac{\mathrm{d}\rho}{\mathrm{d}t_1}\,\mathrm{d}t_1 \ldots \int \frac{\mathrm{d}\rho}{\mathrm{d}t_s}\,\mathrm{d}t_s \int_{\Delta_{t_1}} \mathrm{d}\mathbf{x}_1^{(t_1)} \ldots \int_{\Delta_{t_s}} \mathrm{d}\mathbf{x}_1^{(t_s)}\,\tilde{g}_s\right]. \tag{33}$$

3. Basic ingredients for rate equation modelling

3.1. The fractional coverage, Θ

The exclusion probability, introduced in the previous section, can be employed for computing the kinetics of the fractional coverage, Θ, under the following assumptions: (i) the critical size of the nucleus is zero; (ii) the nucleation and growth laws of the clusters are given *a priori*. Under these circumstances the fractional coverage is simply given by

$$\Theta = 1 - P_E(\Delta), \tag{34}$$

where $|\Delta|$, which is a function of time, is the area of the cluster projection on the substrate surface. In the case of circular clusters of radius R, $|\Delta| = \pi R^2$. It stems from point (ii) that the modelling based on equation (34) is suitable for describing film growth governed by the impingement mechanism whatever the shape of the clusters, provided, in the case of anisotropy of their shape, that they are all oriented in the same way [20]. Otherwise, it is mandatory to reckon with the blocking or shielding effects, as was first done by Weinberg and co-workers [21]. In the following, if not explicitly stated, we will consider circular clusters. In equation (34) the time dependence of Θ is due to the nucleation function and to the growth law of the clusters.

Let us begin by considering the simplest application of this approach to the growth of thin films: the nucleation of spatially uncorrelated islands. In this case $\tilde{g}_s = 0 \forall s \geqslant 2$ and $\tilde{g}_1 = 1$; then from equation (33), identifying the continuous parameter t quite naturally with time, we get

$$P_E = \exp(-\Theta_\mathrm{e}) = \exp\left(-\int \frac{\mathrm{d}\rho}{\mathrm{d}t'}\,\mathrm{d}t' \int_{\Delta_{t'}} \mathrm{d}\mathbf{x}\right) = \exp\left(-\pi \int_0^t I_\mathrm{p}(t')R^2(t,t')\,\mathrm{d}t'\right), \tag{35}$$

where $I_\mathrm{p} = \frac{\mathrm{d}\rho}{\mathrm{d}t}$ is the nucleation rate and $\pi R^2(t,t') = |\Delta_{t,t'}|$, $R(t,t')$ is the radius, at running time t, of those nuclei which started growing in the time interval between t' and $t' + \mathrm{d}t'$. Θ_e is the so-called *extended* surface coverage. Thanks to equation (34) we eventually get

$$\Theta(t) = 1 - \mathrm{e}^{-\Theta_\mathrm{e}(t)}. \tag{36}$$

Usually the time dependence of the cluster radius is assumed to be of the form $R \equiv R(t - t')$, and the extended fractional surface becomes the convolution product of the nucleation rate and the cluster growth law. It is at this level that the kinetics embodies the physical quantities which govern the phase transformation.

Equation (36) was first obtained by Kolmogorov [22] and, independently, two years later, by Johnson and Mehl [23] and by Avrami [24] and is called the KJMA model after them [20]. It is worth noting that, on the grounds of the statistical approach outlined in the previous section, the nucleation rate in equation (35) is also comprehensive of those nuclei which are captured by the growing phase before they start growing. These nuclei do not contribute to the phase transformation, yet they must be included in the mathematical definition of Θ_e. They were called 'phantom' nuclei by Avrami. Nevertheless, since only the actual nucleation rate, I_a, is

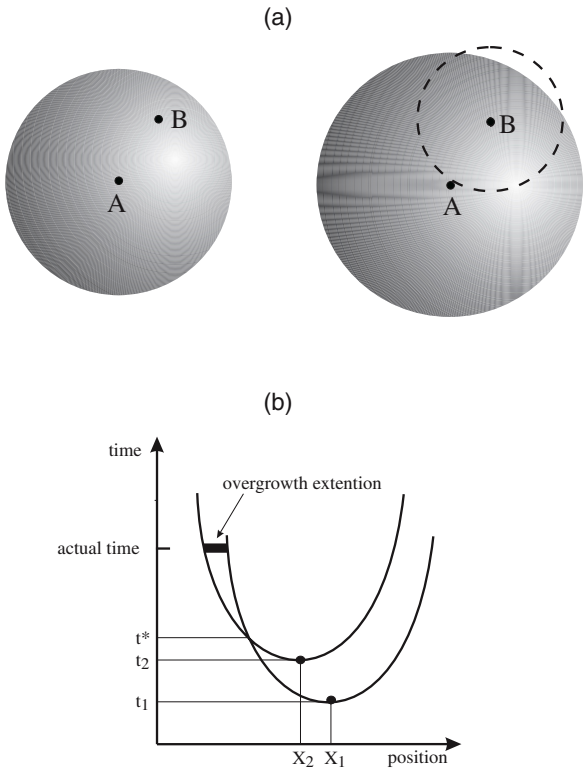

Figure 2. The non-physical overgrowth phenomenon in thin film growth. (a) The actual (A) and the phantom (B) nuclei start growing at times t_1 and $t_2 > t_1$, respectively. The KJMA theory is unsuitable for describing kinetics where the overgrowth phenomena are allowed. (b) Overgrowth event of a phantom nucleus in the case of a parabolic growth law. The actual nucleus located at x_1 starts growing at time t_1 and the phantom nucleus located at x_2 starts growing at time t_2. The overgrowth occurs at time t^* at the intersection of the two parabolas. The segment that joins the two intersections between a parabola and a line parallel to the x-axis represents the grain size at the given time. The extension of the overgrowth is also highlighted at the actual time.

accessible by experiment, it is beneficial to write the extended surface in terms of this rate. As shown in [25], in the case of a random distribution of nuclei the 'phantom-included' nucleation rate is equal to

$$I_{\mathrm{p}}(t) = \frac{I_{\mathrm{a}}(t)}{1 - \Theta(t)} \tag{37}$$

and the kinetics equation (36) becomes an integral equation for the fractional surface coverage, $\Theta(t)$. Moreover, the importance of phantoms is emphasized by the constraint their existence imposes on the cluster growth law. Indeed it happens that for growth laws satisfying the condition $\dot{r}(t-t') < \dot{r}(t-t'')$ with $t' < t''$, a phantom cluster could overtake the 'real' cluster that covers it. This unphysical phenomenon is called 'phantom overgrowth' (figure 2). As a consequence, this kind of growth law does not fall within the class of those treatable using the KJMA model [25]. However, as we will discuss below, the limit of the theory, determined by the phantom overgrowth, can be overcome by facing the kinetic problem at a higher level, namely by treating the phase transformation as a correlated nucleation problem [26].

The simplest application of equation (35) is related to the simultaneous nucleation case which is expressed by the nucleation rate $I_{\mathrm{p}}(t) = I_{\mathrm{a}}(t) = N_0\delta(t)$, where N_0 stands for the

number of nuclei per unit area and δ for the Dirac delta function. The kinetics reduces to the function

$$\Theta(t) = 1 - \mathrm{e}^{-\pi N_0 R^2(t)}. \tag{38}$$

For a cluster radius which evolves according to a power law of the sort $R(t) = vt^n$, the KJMA formula reduces to the stretched exponential

$$\Theta(t) = 1 - \mathrm{e}^{-at^m}, \tag{39}$$

where $a = \pi N_0 v^2$ and $m = 2n$. By using the power growth law, a similar expression is also obtained for constant nucleation rate.

The KJMA kinetics has been employed for describing experimental kinetics of thin film growth. One of its first applications to surface science dates back to 1974 and is due to Holloway and Hudson [27]. They studied the oxidation of the nickel (100) surface by means of Auger electron spectroscopy (AES), low energy electron diffraction (LEED) and techniques based on measurements of the work function. The fractional coverage that was determined through the intensity of the 507 eV oxygen Auger line, exhibits the typical *sigmoidal* behaviour as a function of oxygen exposure. In particular, for cylindrical islands the following relation holds: $\Theta = \frac{I_{\mathrm{AES}} - I_c}{I_n - I_c}$, I_c and I_n being, respectively, the signals from the uncovered portion of the substrate and from n layers of NiO, which is also in appropriate units the (time independent) height of the islands. The authors describe the kinetics in the framework of the Dirac delta nucleation and, by this means, compute the nucleus density and the growth rate. The latter quantity has been modelled by considering the growth kinetics to be limited by either the surface diffusion of adatoms or the capture of oxygen molecules at the perimeter of the islands. For both cases they found $R(t) = vt^2$ which leads, by means of an Arrhenius plot, to the determination of the activation energy for cluster growth which, in turn, is proportional to the difference between the diffusion and desorption activation energies. Behm *et al* by means of LEED intensity measurements performed as a function of time were able to establish that the oxygen induced (2×1) reconstruction of Ni(110) proceeds through nucleation and growth and that the time evolution is described by equation (39), finding $m = 0.3$ [28].

An experimental study on the kinetics of the fractional coverage of diamond film at a solid substrate based on the KJMA model has been reported in [29]. Synthetic diamond was grown on a deformed Si surface by using the hot filament CVD technique which employs a mixture of CH_4 and hydrogen. Diamond formation occurs via the Volmer–Weber mechanism since diamond has the highest surface energy among known materials. Via scanning electron microscopy analysis it was also established that the growth is governed by impingement. The study presented in [29] is quite comprehensive in that it reports on the nucleation and fractional coverage kinetics, on the correlation degree of the nuclei as well as on the kinetics of the island perimeter. The main results of this experiment are shown in figure 3. In panel (a) we report the nucleation kinetics which clearly indicates that the nucleation process comes to an end in a time much shorter than that for film growth. This implies that the nucleation rate can be well approximated by a Dirac delta function. The microscopic growth law of the diamond cluster is reported in panel (b). In particular, both the maximum and the average equivalent diameters of diamond crystallites, as obtained from the size distribution functions of well separated particles, are shown. The cluster radius increases linearly in time. In panel (c) we show the statistical analysis that is aimed at determining whether or not the diamond nuclei are distributed at random throughout the substrate surface. In panel (c) the full line is the Poisson function computed using the average number, m, of nuclei in a 'sampling circle' whose radius was chosen to be $\frac{1}{\sqrt{N_0}}$, N_0 being the nucleation density. The reliability of the Poisson distribution has been confirmed by a χ^2 test, and with it the application of the KJMA

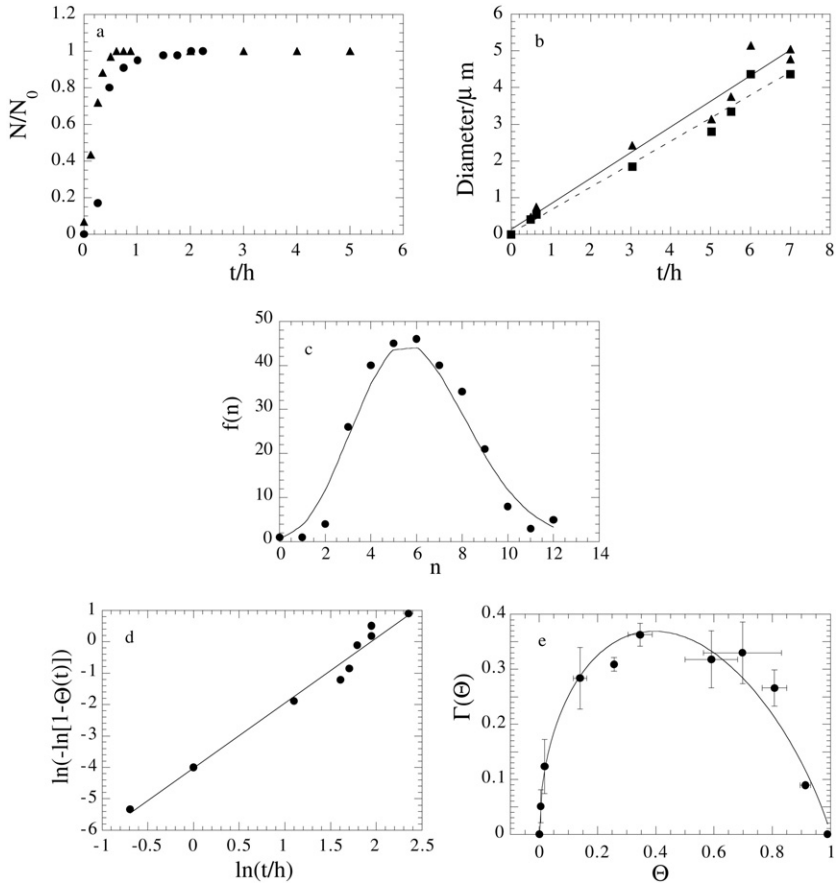

Figure 3. Analysis of experimental data on diamond nucleation and growth at the Si(100) surface by the CVD technique. (a) Nucleation kinetics for 1 h (triangles) and 3 h (circles) deposition time. (b) Microscopic growth law for both the maximum (triangles) and the average (squares) equivalent diameter as obtained from the analysis of the size distribution function of diamond crystallites. (c) Histogram of the nucleation events within a sampling disc of radius equal to the average distance among nuclei. The solid line is the curve expected in the case of a Poissonian distribution of nuclei as evaluated by using the experimental mean value of n. (d) Avrami plot of the fraction of surface covered by diamond, Θ. For the KJMA model this plot is a straight line. (e) Total perimeter of the film, Γ, as a function of surface coverage. The solid line is the best fit of equation (40) to the experimental data.

model. The Avrami plot of the fractional surface coverage, namely $\ln(-\ln[1-\Theta])$ versus t, is shown in panel (d). From the slope of this curve the growth law of the cluster is obtained and it is found to be in excellent agreement with the direct measurement reported in panel (b). In the last panel we show the kinetics of the total perimeter of the diamond film, per unit of substrate area. In the framework of the KJMA method, it can be computed, analytically, as a function of the surface coverage [30], and in the particular case of simultaneous nucleation the kinetics depends upon nucleation density only, according to the relationship

$$\Gamma(\Theta) = \sqrt{4\pi N_0}(1-\Theta)\,[-\ln(1-\Theta)]^{1/2}\,. \tag{40}$$

According to equation (40) the perimeter is maximum at $\Theta = 1 - \mathrm{e}^{-1/2} \simeq 0.39$. In figure 3 panel (e) the continuous line is the best fit of equation (40) to the experimental points. From

the fitting parameter the nucleation density of diamond has also been obtained and it is found to be in good agreement with the value determined from the direct measurements (figure 3 panel (a)). It is worth mentioning, in passing, that in general the film perimeter can be expressed as a series expansion in terms of the f-function [31]. This formulation can be used to describe the kinetics of island perimeter in the case of spatially correlated nuclei.

Incidentally, the stochastic process of dots has been recently used for modelling film roughness and the height–height correlation function for different hillock shapes and different nucleation modes [32]. The authors found that the surface height distribution is asymmetric and the height–height correlation function is non-Gaussian.

Let us now pass to considering the more general case of non-random nucleation. The general expression for the fractional coverage is obtained by simply combining equations (33) and (34). In order to obtain a mathematical expression similar to that for the Poissonian case, it is beneficial to define a function, γ, as the ratio between the exponent of equation (34) and the extended surface coverage. The fractional coverage therefore reads

$$\Theta = 1 - \mathrm{e}^{-\gamma\Theta_\mathrm{e}}. \tag{41}$$

Obviously in the random case $\gamma = 1$, whereas in the correlated one the γ factor is different from one and depends upon the nucleation rate, m-dot correlation functions and Θ_e. Incidentally, although not necessarily in 2D, other approaches have been proposed for treating phase transition kinetics in the case of non-random nucleation. In this respect, among others, we quote the papers by Trofimov and Hermann for 3D and 2D transitions, [33, 34] respectively.

To begin with, we confine our attention to the simultaneous nucleation case which stems from considering, in the stochastic approach, a single class of indistinguishable dots (see section 2.1). Furthermore, the system is considered to be homogeneous and isotropic which implies $g_1 = N_0$ and $g_m = g_m(|\mathbf{r}_2 - \mathbf{r}_1|, \ldots, |\mathbf{r}_m - \mathbf{r}_1|)$. Combining equations (21), (34) and (41), the truncation of the γ expansion to the second-order term in the correlation functions leads to [35, 36]

$$\gamma = 1 + \frac{\Theta_\mathrm{e}}{2} - \frac{N_0^2}{2\Theta_\mathrm{e}} \int_0^R 2\pi r \,\mathrm{d}r \int_0^{2\pi} \mathrm{d}\theta \int_0^{\eta(r,\theta)} g(\xi)\xi \,\mathrm{d}\xi, \tag{42}$$

where the two-dot correlation function has been expressed in terms of the radial distribution function, $g(\xi)$, according to the relationship $g_2(\xi) = N_0^2[g(\xi) - 1]$. In equation (42), $\eta(r,\theta) = r\cos\theta + (R^2 - r^2\sin^2\theta)^{1/2}$ and $\Theta_\mathrm{e} = \pi N_0 R^2$. The fractional coverage has been computed for nuclei correlated according to the hard core model which implies that the distance among nuclei cannot be shorter than a given value, say R_hc. The lowest order term of the radial distribution function is given by

$$g(\xi) = H(\xi - R_\mathrm{hc}), \tag{43}$$

where H is the Heaviside function and R_hc the hard core diameter, i.e. the radius of the circular region, surrounding each nucleus, where nucleation is prevented (figure 4). The approximation equation (43) holds for low values of the surface density of nuclei [37], a condition which is usually satisfied in thin film growth. The γ exponent is a function of Θ_e and of $\Theta^* = \pi N_0 R_\mathrm{hc}^2$, this last term being a possible measure of the degree of correlation among the nuclei. Indeed, Θ^* has the meaning of extended area with nucleation precluded, which is larger than the area where nucleation is actually prevented because of the overlaps among excluded zones of the nuclei. For the hard core model the validity of the analytical approach has been verified through computer simulations over the range $0.2 < \Theta^* < 1.5$ where the γ factor has been obtained through numerical integration of equation (42). The results are displayed in figure 5 for $\Theta^* = 0.2$ (panel (a)), $\Theta^* = 0.7$ (panel (b)), $\Theta^* = 1.5$ (panel (c)); the KJMA solution ($\Theta^* = 0$) has also been reported. The agreement is excellent for $\Theta^* = 0.2$ and 0.7 and

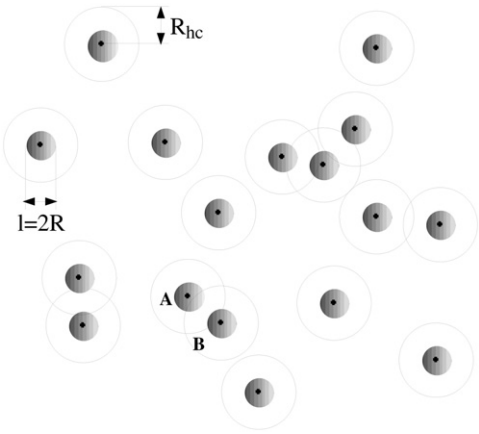

Figure 4. Sketch of the nucleus arrangement spatially correlated according to the hard core model.

more than satisfactory for $\Theta^* = 1.5$. In [35] an analytical expression for γ has been achieved by simply decoupling the integrals over ξ from those over r and θ, namely by setting $\eta = R$. The γ expression reads

$$\gamma = 1 + \frac{1}{2}\left[\Theta_e H\left(1 - \frac{\Theta_e}{\Theta^*}\right) + \Theta^* H\left(\frac{\Theta_e}{\Theta^*} - 1\right)\right] \tag{44}$$

and, as shown in figure 5, well describes the kinetics over the whole range of the Θ_e values. Apparently, from the mathematical point of view the derivation of equation (44) is not justified, yet it can be accepted to the extent that it reproduces computer simulations. Once its excellence is recognized, it undoubtedly has the merit of being easy to employ in the treatment of experimental data. The evaluation of the γ exponent by considering the term of order N_0 in the expansion of the radial distribution function indicates that that contribution is negligible [35]. On the other hand, for high correlation degrees ($\Theta^* = 1.5$) the discrepancy between the analytical solution and the computer simulation, in the region of high coverages, is ascribed to the contribution of the m-dot correlation functions with $m > 2$.

The knowledge of the probability function $P_E(\Delta)$ can be extremely useful for solving kinetic problems which are not linked, apparently, to the physical processes of nucleation and growth. In fact, the continuum space random sequential adsorption (RSA) and the Tobin process [38] can be successfully tackled in the framework of the stochastic approach discussed already. The RSA process consists in throwing discs, at random, onto a surface where overlap among discs is not permitted. Such a process models the random non-ideal adsorption of molecules at a solid surface when interaction among molecules behaves according to the hard disc potential. It is evident that a coverage value exists for which there is no more room available for accommodating other discs (jamming point). In other words the kinetics ends for a coverage value lower than one. The Tobin process has been formulated in 1974 in the ambit of thin film growth and refers to the model case of non-simultaneous nucleation and instantaneous growth up to a finite value of the disc radius. Tobin's process is the equivalent of throwing discs at random onto a flat surface and removing any disc whose centre falls into an area already occupied by previously thrown discs. The kinetic problem of both RSA and Tobin's processes consists in determining the fraction of substrate surface covered by molecules and by film, respectively.

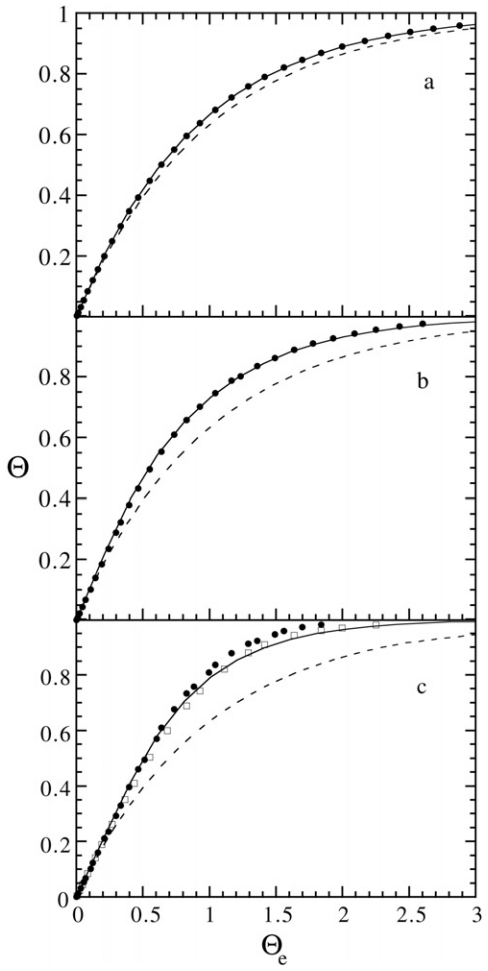

Figure 5. Comparison between Monte Carlo simulations (dots) and analytical solutions in the case of simultaneous nucleation. The spatial correlation among nuclei has been described according to the hard core model for $\Theta^* = 0.2$ (panel (a)), $\Theta^* = 0.7$ (panel (b)) and $\Theta^* = 1.5$ (panel (c)). Full symbols are the output of the computer simulations performed, for $R(t) = at^n$ at $a = n = 1$. The curves computed using equation (44) are displayed as open symbols. The continuous line is the analytical solution obtained by considering only the Heaviside term in the $g(\xi)$ expansion. In the cases $\Theta^* = 0.2$, 0.7 full lines and open symbols coincide. The dashed lines represent the KJMA solution.

As far as the RSA kinetics is concerned we note that equation (21) can be employed for computing the adsorption rate of discs of diameter σ. In fact the adsorption rate is

$$\frac{\mathrm{d}N}{\mathrm{d}t} = FP_E(\Delta_\sigma) = F\mathrm{e}^{-\gamma\Theta_\mathrm{e}}, \tag{45}$$

where F is the flux of discs which impinge at the surface, $\frac{\mathrm{d}N}{\mathrm{d}t}$ is the adsorption rate, $P_E(\Delta_\sigma)$ is the probability that an incoming disc finds enough room to be adsorbed and $|\Delta_\sigma| = \pi\sigma^2$. It is evident that this is nothing but a problem of simultaneous correlated nucleation according to a hard disc model with $R_\mathrm{hc} = \sigma$. Consequently, in terms of the previously defined Θ_e and Θ^* quantities, the continuous space RSA implies $\Theta_\mathrm{e} = \Theta^* = \pi N\sigma^2$ where the surface coverage

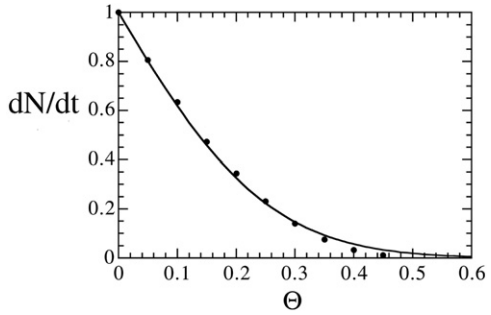

Figure 6. Kinetics of continuous space random sequential adsorption. The adsorption rate for hard discs is plotted as a function of surface coverage ($F = 1$). The analytical solution equation (46) (full line) has been compared with the numerical simulation (dots).

of the adsorbed disc is $\Theta = N\pi\sigma^2/4$. By employing equation (44) for the γ exponent one ends up with

$$\frac{\mathrm{d}N}{\mathrm{d}t} = F\exp\left[-4\Theta\left(1+2\Theta\right)\right] \tag{46}$$

and then

$$\frac{\mathrm{d}\Theta}{\mathrm{d}L} = \exp\left[-4\Theta\left(1+2\Theta\right)\right], \tag{47}$$

where $L = \pi\sigma^2 Ft/4$. As displayed in figure 6 the equation (46) is in very good agreement with the MC simulation, except in the high coverage regime that is characterized by very low adsorption rates [39]. Equation (46) is not suitable for studying the complete behaviour of the kinetics; indeed it does not predict any maximal coverage. This issue is better tackled by employing an f-function representation of the Q probability (equation (17)), for in this case only the integrals up to $n = 5$ have to be retained [39–41]. The expression for the $\frac{\mathrm{d}\Theta}{\mathrm{d}L}$ rate is a polynomial and the adsorption process is therefore characterized by an asymptotic coverage value, usually called the jamming point. For instance, expansion of $P_E(\Delta_\sigma)$ in terms of f-functions up to the second-order term f_2 considering only the Heaviside contribution to the radial distribution function gives

$$\frac{\mathrm{d}\Theta}{\mathrm{d}L} \approx 1 - 4\Theta + 8(1-\alpha)\Theta^2, \tag{48}$$

where $\alpha = 1 - 3^{3/2}/4\pi$ is referred to as the impingement factor [42]. However, truncation of the series to the second-order term is not accurate for determining the jamming point; in fact it provides a saturation point of 0.35 against the exact value 0.547 [43].

Let us now briefly dwell upon Tobin's process. The constraint to which the nucleation event is subjected clearly indicates that, in this case also, we are facing a hard core correlation problem with $R_{\mathrm{hc}} = R = \sigma/2$, σ being the disc (i.e. nucleus) diameter. The fraction of transformed surface is therefore given by equation (41) where the extended surface is now $\Theta_{\mathrm{e}} = \pi N(t)\sigma^2/4$, $N(t)$ being the disc density at time t. It is worth noting the analogies of and differences between the RSA and Tobin processes: (i) the hard core radius differs by a factor of 2; (ii) in Tobin's process, at variance with the RSA, due to the overlap among discs the fraction of transformed surface is not equal to the extended surface. The application of equation (41) for describing Tobin's process has been thoroughly discussed in [44], also in relation to the approximate solutions previously put forward. As for the RSA, in this case also the integrals of functions f_n with $n > 5$ are identically nil. Consequently both in the RSA and

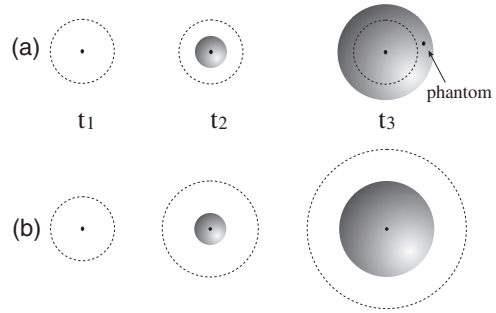

Figure 7. Pictorial view of hard core correlations in thin film growth for three values of the running time. In case (a) nucleation is not allowed within the correlation length, $R_{\rm hc}$, from the nucleus centres (dashed circles). As the running time increases the nucleus radius becomes larger than $R_{\rm hc}$ and phantom nucleation is possible (running time t_3). In case (b) nucleation is forbidden both in the already transformed surface and in an annular ring of thickness $R_{\rm hc}$ drawn around each nucleus. In this case phantom nucleation is not included in the analytical model.

the Tobin processes the fraction of covered surface admits a saturation point, that is $\frac{\mathrm{d}\Theta}{\mathrm{d}t}$ is zero at finite values of Θ which are the zeros of the P_E. In summary, Tobin's process for discs of radius R is stochastically 'equivalent' to an RSA process for discs of radius $R/2$.

Let us now pass to broaching thin film growth in the case of non-simultaneous nucleation of correlated nuclei. In these circumstances it is compulsory to resort to the exclusion probability computed in section 2.2 for distinguishable classes of dots. In fact, the nuclei start growing at any time, t', in the interval $[0, t]$, under a growth law given *a priori*: $R = R(t, t')$, so we can classify, and therefore distinguish, cluster sets in terms of their radius: the time of birth, t', becomes, in the continuum limit, the class index. In this event, the nuclei (dots) are distinguishable because of their size. The fractional coverage is obtained by computing the probability that no nuclei belonging to any of the t' classes appear in the area $\Delta_{t,t'} = \pi R(t, t')^2$. By making use of the equation (33), identifying, quite naturally again, the parameter t with time, thanks to equations (41) and (34) it is possible to show, retaining terms up to the second order in the correlation functions [18, 19], that

$$\gamma = 1 + \frac{1}{2}\Theta_{\rm e} - \frac{1}{2\Theta_{\rm e}} \int_0^t I(t')\,\mathrm{d}t' \int_0^t I(t'')\Phi(t', t'')\,\mathrm{d}t'', \tag{49}$$

where the $\Phi(t', t'')$ reads

$$\Phi(t', t'') = \int_0^{R(t,t')} 2\pi r\,\mathrm{d}r \int_0^{2\pi} \mathrm{d}\theta \int_0^{\eta[R(t,t''),r,\theta]} g(\xi, t', t'')\xi\,\mathrm{d}\xi, \tag{50}$$

in which the translational invariance of the system was exploited. The function $g(\xi, t', t'')$ is the radial distribution function of a pair of nuclei belonging to the t' and t'' classes. Depending upon the correlation function, several processes can be investigated. In what follows we report on the cases (a) and (b) displayed in figure 7. Case (a) concerns the hard core constant correlation length. It is measured from the nucleus centre and within it nucleation is forbidden. Once the cluster radius overtakes the correlation distance, nucleation of phantom clusters becomes possible. The second case ((b) in figure 7) deals with the more physical situation where nucleation is forbidden both in a region already transformed by the new phase and, possibly, in an annular ring of constant thickness around each nucleus. It goes without saying that other correlation mechanisms can be devised, for instance, the dependence of the thickness of the annular ring upon the cluster radius.

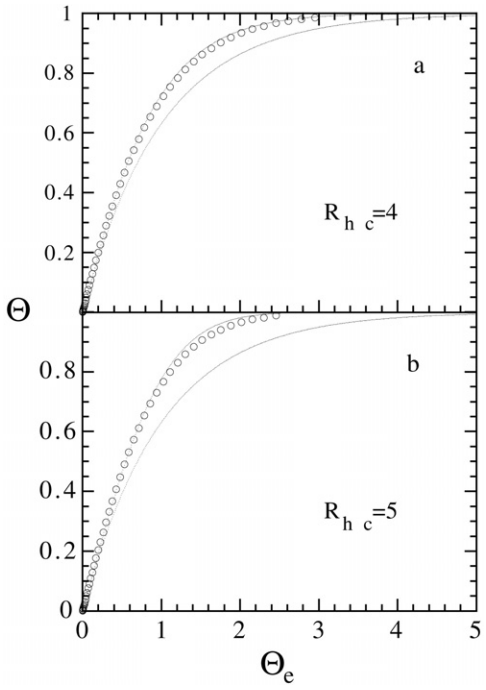

Figure 8. Comparison between the Monte Carlo simulations (open symbols) and the analytical solutions (equations (41), (51)) in the case of constant nucleation rate. The spatial correlation among nuclei has been described according to the hard core model where $R_{\rm hc}$ denotes the hard core radius. The KJMA solution is also shown.

As far as the first case is concerned, the correlation function is given, subject to the limits already discussed, by equation (43). The γ factor has been computed, analytically, in the case of constant rates of both nucleation and cluster growth and, as for the simultaneous nucleation case, the integrals (equation (50)) have been arbitrarily decoupled by using the condition $\eta = R(t, t'')$, giving[4]

$$\gamma(\Theta_{\rm e}, \Theta^*) = 1 + \frac{\Theta_{\rm e}}{2} H\left(1 - \frac{3\Theta_{\rm e}}{\Theta^*}\right) + \frac{1}{2}\left[\Theta^* - 2\Theta_{\rm e}\left(\frac{\Theta^*}{3\Theta_{\rm e}}\right)^{3/2}\right] H\left(\frac{3\Theta_{\rm e}}{\Theta^*} - 1\right) \tag{51}$$

where $\Theta^* = I\pi R_{\rm hc}^2 t$ is the 'extended area' with nucleation precluded and $R_{\rm hc}$ is the hard core radius. The validity of equations (41), (51) has been verified through computer simulations. The simulation has been performed on a 300×300 square lattice where in any iteration 250 new nuclei start growing. The comparison among the analytical and the numerical calculations is shown in figure 8 for two values of the hard core radius. As appears also in this case, the agreement between the analytical model and the simulation is more than satisfactory.

As regards case (b) the zero-order radial distribution function is given by

$$g(\xi, t', t'') = H[\xi - \big(R(t'' - t') + R_{\rm hc}\big)], \tag{52}$$

[4] As we have underlined in discussing the simultaneous nucleation case, the benefit of 'decoupling' the integral resides in its capacity for reproducing the experimental and/or numerical data. Since the Φ function is symmetric in the t', t'' arguments, the integral equation (49) is also equal to $\gamma = 1 + \frac{1}{2}\Theta_{\rm e} - \frac{1}{\Theta_{\rm e}} \int_0^t I(t')\,{\rm d}t' \int_0^{t'} I(t'')\Phi(t', t'')\,{\rm d}t''$ which, once decoupled, leads to $\gamma(\Theta_{\rm e}, \Theta^*) = 1 + \frac{\Theta_{\rm e}}{2} H(1 - \frac{3\Theta_{\rm e}}{\Theta^*}) + \frac{\Theta^*}{12}[3 - (\frac{\Theta^*}{3\Theta_{\rm e}})^2] H(\frac{3\Theta_{\rm e}}{\Theta^*} - 1)$ which differs from equation (51). Nevertheless the difference between the two is negligible and they can be used interchangeably.

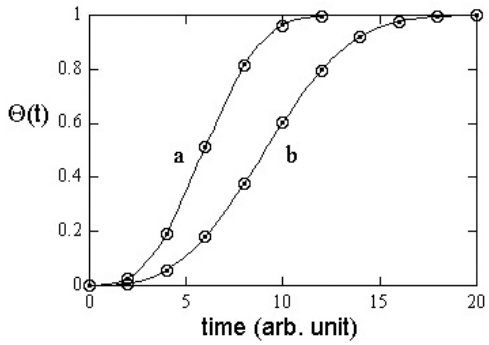

Figure 9. Kinetics of thin film growth in the case of random distribution of nuclei and constant nucleation rate (KJMA kinetics). The points represent the classical KJMA solution which implies the inclusion of the virtual nucleation throughout the whole space in the computation of Θ_e. The open symbols are the kinetics of the phase transition obtained by using the actual nucleation; in fact the actual nuclei are spatially correlated. The parameter values are (equation (39)): $a = 0.\bar{3} \times 10^{-2}$ (curve a), $a = 1.\bar{1} \times 10^{-3}$ (curve b) and $m = 3$.

where the growth law is assumed to be in the form $R = R(t - t')$. It is worth remarking that such a correlation does not allow phantom nucleation. Therefore, since in the limit $R_{hc} = 0$ the growth process reduces to the one solved by KJMA, the approach of section 2.2 together with equation (52) reproduces the KJMA kinetics by using the actual nucleation (phantoms are not included). This result is particularly important not only because it uses the actual nucleation rate that is accessible by experiment, but also because it can be used for any growth law. In contrast, as anticipated above, the KJMA theory cannot be applied to any kind of growth law. Reference [26] is devoted to illustrating that the classical KJMA solution is obtained by dealing with correlated nucleation which obeys equation (52) with $R_{hc} = 0$. In the correlated approach the integral equation (49) has to be computed, which includes the actual nucleation rate. Nevertheless it is readily evaluated by combining equation (37) and equation (36). The computation has been performed for square clusters and for the following pair distribution function:

$$g(\mathbf{r}, t', t'') = W(x, y, l_{1,2}), \tag{53}$$

where W is the two-dimensional square well of side $l_{1,2}$, $\mathbf{r} \equiv (x, y)$, $l_{1,2} = l(t'' - t') = (t'' - t')v$, l being the cluster side and v the growth velocity. The solutions of the KJMA problem obtained by dealing with the correlation among actual nuclei and the classical KJMA kinetics have been compared in figure 9: the agreement is excellent.

3.2. The adatom lifetime

The exclusion probability can be also used for computing a physical quantity that is indispensable for modelling thin film growth through the rate equation method: the *adatom lifetime* (see also section 4). In film growth ruled by the diffusion mechanism the adatom performs a random walk on the surface before being captured by the islands of the new phase. The average time elapsed between the arrival of the monomer at the surface and its capture is the lifetime of the adatom, τ. The computation of τ is performed using a stochastic approach which relies on the definition of the probability $P[t', t, \Theta(t'), \Theta(t)]$ that an atom that landed on the surface at time t' does not suffer any capture event until time t. Since $-\partial_t P(t)$ is just the probability that the adatom will be captured in the time interval $[t, t + \mathrm{d}t]$, the adatom lifetime

results as

$$\tau = \frac{1}{\int_{t'}^{\infty} \mathrm{d}P(t)} \int_{t'}^{\infty} t \, \mathrm{d}P(t). \tag{54}$$

The computation can be considerably simplified by resorting to the so-called QSA (quasi-static approximation). Under this approximation, during the lifetime of the adatom the fractional coverage does not change and can be set equal to the coverage at the monomer landing time. As a consequence, P depends upon Θ parametrically and, for each value of the parameter, the landing time can be set equal to zero, so that [45]

$$\tau(\Theta) = \frac{1}{P(0;\Theta)} \int_{0}^{\infty} P(t;\Theta)\, \mathrm{d}t, \tag{55}$$

where $P(0;\Theta) = 1 - \Theta$ is the probability that the adatom, at the landing time, be on the uncovered portion of the substrate. The following step is to determine the function $P(t;\Theta)$. The simplest case that can be treated analytically is simultaneous nucleation without monomer re-evaporation.

Two advantages stem from these hypotheses, namely that the consumption of monomers is only due to island growth and the clusters all have the same size. A neat approach for solving this problem is exploiting the random walk of the *dressed* adatom. By 'dressed' we mean that the monomer in its random walk carries with it an area equal to that of the cluster at time t. In this way the probability that the dressed adatom met a nucleus is the same as the probability that the adatom is captured by any cluster (figure 10). It is evident that in the time interval $[0, t']$ during its roaming on the surface the dressed adatom will cover a portion of the surface of area, say, $|\Delta_{l,t'}|$ where l is the cluster side. Consequently, the probability that we are searching for is just equal to the exclusion probability on the region $\Delta_{l,t'}$, i.e.

$$P(t') = P_E(\Delta_{l,t'}), \tag{56}$$

which also depends, as anticipated, on the running time through the cluster side $l = l(t)$. The question is how to determine the region $\Delta_{l,t'}$. The simplest and most reasonable way to answer this question is to consider a square region whose side is proportional to the random walk standard deviation [45, 46]: $l(t) + 2p\sqrt{2Dt'}$, p being a dimensionless factor. The adatom lifetime becomes

$$\tau = \frac{1}{1-\Theta} \int_{0}^{\infty} P_E \left\{ \left[l(t) + 2p\sqrt{2Dt'} \right]^2 \right\} \mathrm{d}t'. \tag{57}$$

For a Poissonian distribution of nuclei the computation is straightforward and leads to [45]

$$\tau' = DN_0\tau = \frac{[-\ln(1-\Theta)]}{4p^2(1-\Theta)} \int_{0}^{\infty} (1-\Theta)^{(1+\xi)^2} \, \mathrm{d}\xi, \tag{58}$$

which indicates that the dimensionless lifetime, τ', is a universal function of the surface coverage. As far as the p parameter is concerned it has been estimated by fitting the analytical result for the random case (equation (58)) to the lifetime as obtained by Monte Carlo simulations [45]. The computer simulations indicate that p depends, weakly, on the fractional coverage, with an average value of $p = 0.9$. On the basis of the conjecture according to which the p quantity is a property of the random walk, the same p value can also be retained for modelling the correlated case.

The analytical computation of the adatom lifetime in the case of simultaneous nucleation of correlated square nuclei has been recently presented in [47]. The correlation among nuclei is described in the framework of the hard core model where the radial distribution function is

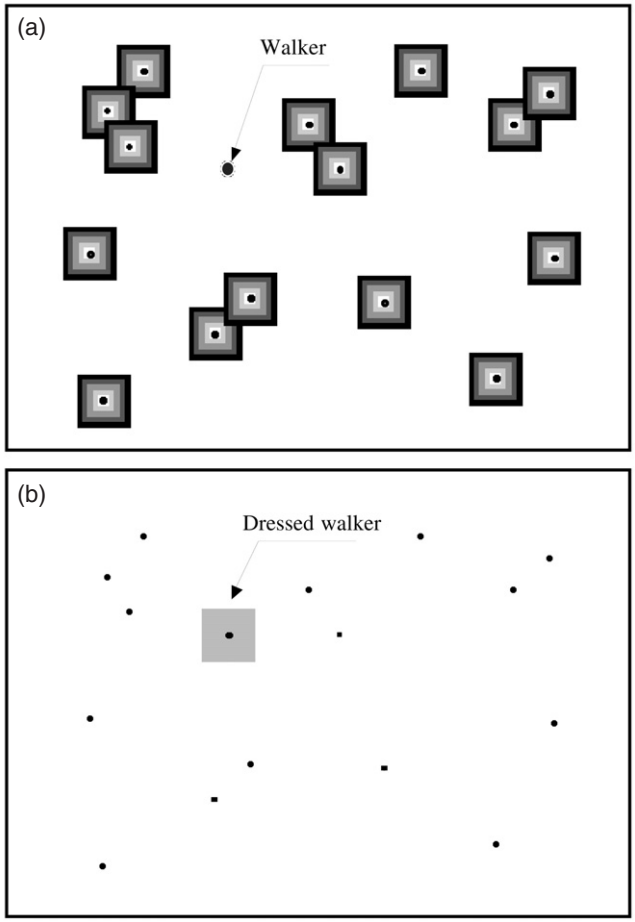

Figure 10. Sketch of an adatom (walker) wandering on a surface that is covered by islands (panel (a)). The probability that the walker be captured by a cluster can be computed by considering the stochastic process of the capture of the *dressed* adatom (panel (b)) by a nucleation centre.

approximated by a square well of side l_c: $g(x, y) = W(x, y; l_c)$. The γ term which enters in the probability function, $P_E(|\Delta_{l,t'}|) = \exp(-\gamma N_0 |\Delta_{l,t'}|)$, is given according to

$$\gamma = 1 + \frac{X_e}{2} - \frac{N_0^2}{2X_e}\Gamma(L, l_c) \tag{59}$$

with

$$\begin{aligned}\Gamma(L, l_c) &= 4\int_0^{L/2} dx' \int_0^{L/2} dy' \int_{-(L/2+x')}^{L/2-x'} dx \int_{-(L/2+y')}^{L/2-y'} W(x, y; l_c)\, dy \\ &= 2\left\{\left(L - \frac{l_c}{2}\right)^2 \left[L^2 - \frac{1}{2}\left(L - \frac{l_c}{2}\right)^2\right]\right\} H\left(L - \frac{l_c}{2}\right),\end{aligned} \tag{60}$$

where $L = l(t) + 2p\sqrt{2Dt'}$ and $L^2 = |\Delta_{l,t'}|$. Also in the correlated case it is possible to define the dimensionless lifetime, τ', as already done in equation (58). Clearly, the presence of correlation between nuclei introduces an extra dependence of τ' on the extended excluded

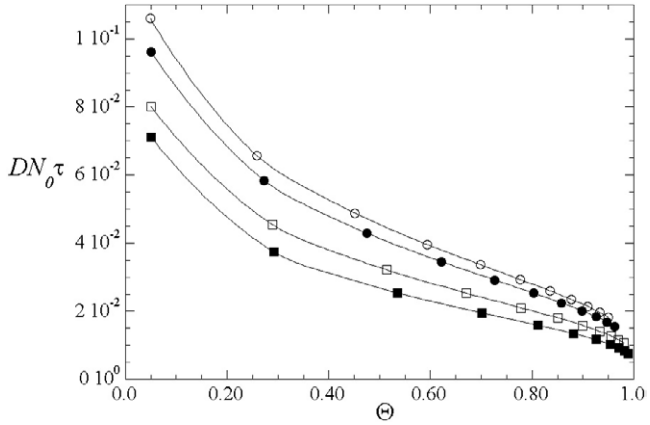

Figure 11. The adatom lifetime, normalized to the diffusion coefficient and to the nucleus density, is shown as a function of surface coverage: open circles, $\Theta^* = 0$; solid circles, $\Theta^* = 0.2$; open squares, $\Theta^* = 0.8$; solid squares, $\Theta^* = 1.5$.

area, that is on $\Theta^* = N_0 l_c^2$. In other words, the lifetime is a function of $\Theta_e = N_0 l^2$, Θ^* and p. However, by exploiting the kinetics of the fractional coverage, $\Theta = \Theta(\Theta_e, \Theta^*)$, the Θ_e coverage can be easily expressed in terms of both actual coverage and extended excluded area. In figure 11 $\tau'(\Theta, \Theta^*, p)$ is shown as a function of Θ at $p = 0.9$ and for several values of the correlation degree, Θ^*. For $\Theta^* = 0$ the random case is recovered where the evolution of the fractional coverage is given by the KJMA theory [24]. Figure 11 shows that for a given Θ value the adatom lifetime is a decreasing function of Θ^*. This result can be justified on the basis of the morphology of the film, for overlaps among clusters are expected to be less effective as the correlation degree of the system increases. In the random case this implies a distribution of islands which allows for the presence of larger uncovered regions of the substrate, when compared to the correlated nucleation. In other words, the transformed phase is expected to be more homogeneous for larger Θ^* values.

3.3. Coalescence and impingement

One of the problems that occurs during the film formation characterized by nucleation and growth is the collision among clusters. This issue must be taken into account in a scheme of description based on rate equations whenever it is intended to study the film evolution over the entire range of coverage, i.e. $0 \leqslant \Theta \leqslant 1$. The rate equation approach has been frequently employed to study the early stage of film formation, namely the nucleation stage. For this reason, in almost all the work devoted to this, terms linked to collision are missing from the equations. However, it is worth stressing that ignoring the contribution of cluster collision and, at the same time, achieving a good description of the kinetics is strictly connected to the presence of spatial correlation among nuclei and/or between nuclei and islands. As a matter of fact, if the nucleation were Poissonian the rate of collision would not be negligible even at the very beginning of the film formation. The reason resides in the fact that the probability of finding two nuclei very close each other is not negligible at all for a Poisson process.

It goes without saying that as the kinetics proceeds, cluster collision is unavoidable, leading to a reduction of the number of islands. We distinguish two extreme cases: coalescence and impingement. By the former we mean a collision process followed by a redistribution of matter with shape and mass conservation. The latter, instead, describes a collision process where no

matter redistribution or relaxation occur at all; in other words, when two or more clusters impinge they retain their individuality.

Our aim is to determine the law which governs the reduction of the island number as a function of surface coverage Θ. To this end we will employ a stochastic approach under the following hypotheses:

(a) there are N_0 dots per unit area (dot, centre of cluster and nucleus are synonymous);
(b) the dots are distributed at random and homogeneously throughout the space;
(c) all of the clusters have the same size whatever the value of Θ.

Moreover, we add a further assumption, in order to make calculations simpler:

(d) clusters are squares.

If $N(\Theta)$ is the number of islands at Θ, we may write

$$N_0 = \sum_k k N_k(\Theta), \tag{61}$$

$$N(\Theta) = \sum_k N_k(\Theta), \tag{62}$$

where $N_k(\Theta)$ is the fraction of islands made up of k clusters; such an island will be referred to as a k-island. Equations (61) and (62) can be rewritten as [48]

$$1 = \sum_k \frac{k N_k(\Theta)}{N_0} \equiv \sum_k P_k(\Theta) \tag{63}$$

$$G(\Theta) = \frac{N(\Theta)}{N_0} = \sum_k \frac{N_k(\Theta)}{N_0} = \sum_k \frac{P_k(\Theta)}{k}. \tag{64}$$

The function $P_k(\Theta)$, defined by equation (63), is *the probability that a cluster belong to a k-island*, while equation (64) can properly be referred to as the *collision series*. Apparently, the next step will be to determine the $P_k(\Theta)'$s. Let us proceed systematically. The origin of the reference frame is located at the centre of a cluster randomly chosen out of the N_0 equivalent clusters of side l. The collision zone of this cluster, i.e. the region within which the centre of one more cluster has to lie in order to collide with it, is the area enclosed in the square of side $2l$, namely A_1. Thus, the probability of having a single isolated cluster is given by

$$P_1(\Theta) = \mathrm{e}^{-N_0 A_1} = \mathrm{e}^{-4N_0 l^2} = (1-\Theta)^4. \tag{65}$$

As far as the $P_2(\Theta)$ evaluation is concerned we must require that, besides a dot at the origin, a second dot lie in the area A_1 at (x, y) within $\mathrm{d}x\,\mathrm{d}y$ and that, concomitantly, no other dots lie within the area $A_2(x, y)$, which is the union of the two collision zones (figure 12). In addition, we have to integrate over the collision zone of the nucleus at the origin, i.e. the square of side $2l$; or, in other words, over all of the possible configurations of two connected clusters:

$$\begin{aligned} P_2(\Theta) &= \int_{A_1} \mathrm{e}^{-N_0 A_2(x,y;\Theta)} N_0\,\mathrm{d}x\,\mathrm{d}y = 4N_0 l^2 \int_{A_1} \mathrm{e}^{-4N_0 l^2 A_2(\xi,\eta;\Theta)}\,\mathrm{d}\xi\,\mathrm{d}\eta \\ &= 4\ln\left(\frac{1}{1-\Theta}\right) \int_{A_1} (1-\Theta)^{4A_2(\xi,\eta;\Theta)}\,\mathrm{d}\xi\,\mathrm{d}\eta, \end{aligned} \tag{66}$$

where $\mathrm{d}x\,\mathrm{d}y = 4l^2\,\mathrm{d}\xi\,\mathrm{d}\eta$ and we have retained the same symbol A_k after having changed the coordinates. Equation (66) can be generalized to evaluate $P_k(\Theta)$ straightforwardly:

$$P_k(\Theta) = \left(4\ln\frac{1}{1-\Theta}\right)^{k-1} \prod_{j=1}^{k-1} \int_{A_j} (1-\Theta)^{4A_k(\{\xi,\eta\};\Theta)}\,\mathrm{d}\xi_j\,\mathrm{d}\eta_j; \tag{67}$$

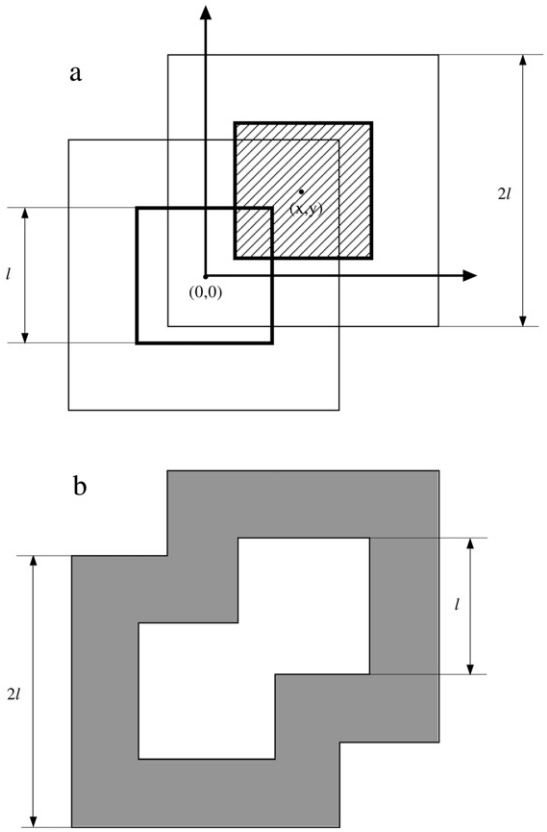

Figure 12. Pictorial view of an island made up of two nuclei located at (0, 0) and (x, y) respectively (panel (a)). The collision zone of a single cluster is also shown in panel (a), whereas the area of the island is evidenced in panel (b) (white area). Note that the collision area of the island is equal to the union of the white and dashed areas.

the integral is performed over all distinct arrangements of the k connected clusters. Although equation (67) settles formally the matter of the collision series, unfortunately it is also evident that it soon becomes unmanageable. In particular, for $k = 4$, owing to the large number of arrangements to take into account, it is already necessary to introduce an approximation. Nevertheless, the comparison between the approximated $G(\Theta)$ up to $k = 4$ and a Monte Carlo simulation demonstrates that the collision series is rapidly convergent and that its incomplete analytical evaluation is a fairly acceptable approximation of the exact kinetics [49]. Moreover, the latter perfectly fits a function of the following kind:

$$G(\Theta) = \mathrm{e}^{-a\Theta - b\Theta^3} \tag{68}$$

when $a = 2.2$, $b = 5.22$. The curve fit is also reported in figure 13.

As regards the coalescence, the reader will find a thoroughly analytical and numerical study in [50]. Here we will just report a simple and only seemingly naive calculation [51].

Let us consider the probability that a square region of side z be not overlapped by clusters, when these possess a side size equal to l; it is

$$P(z; \Theta) = \mathrm{e}^{-N_0(z+l)^2}. \tag{69}$$

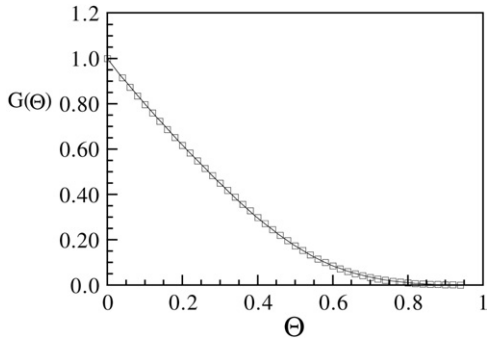

Figure 13. Collision series, $G(\Theta)$, in the case of simultaneous nucleation of square nuclei randomly distributed throughout the space. The kinetics refers to the impingement growth mechanism. The Monte Carlo simulation of the film growth is shown as open symbols; the continuous line is the best fit of equation (68) to the numerical kinetics.

Consequently, the mean side of this empty region, which is also the average value of the edge-to-edge distance among islands, is

$$\bar{z}(\Theta) = \frac{\int_0^\infty z\,\mathrm{d}P}{\int_0^\infty \mathrm{d}P} = \frac{1}{P(0)}\int_0^\infty P\,\mathrm{d}z$$
$$= \frac{1}{\sqrt{N_0}}\frac{1}{1-\Theta}\left(\ln\frac{1}{1-\Theta}\right)^{1/2}\int_0^\infty (1-\Theta)^{(1+\zeta)^2}\,\mathrm{d}\zeta, \tag{70}$$

where $\zeta = \frac{z}{l}$ and $l = \frac{1}{\sqrt{N_0}}(\ln\frac{1}{1-\Theta})^{\frac{1}{2}}$. In particular, as $P(z;0) = \mathrm{e}^{-N_0 z^2}$, from equation (70) it follows that

$$\bar{z}(0) = \sqrt{\frac{\pi}{4N_0}}. \tag{71}$$

The average side of the island when the fraction of covered surface is Θ and N is the number of islands per unit area is

$$\bar{l}(\Theta) = \sqrt{\frac{\Theta}{N}}, \tag{72}$$

while the distance between the centres of the islands, on the analogy of equation (71), can be written as

$$\bar{d} = \sqrt{\frac{\pi}{4N}}. \tag{73}$$

Clearly $\bar{z}(\Theta) = \bar{d} - \bar{l}(\Theta)$, and using equations (70), (72) and (73) we eventually obtain

$$\frac{N(\Theta)}{N_0} = \left(\frac{\sqrt{\frac{\pi}{4}} - \sqrt{\Theta}}{W(\Theta)}\right)^2, \tag{74}$$

where

$$W(\Theta) \equiv \frac{1}{1-\Theta}\left(\ln\frac{1}{1-\Theta}\right)^{1/2}\int_0^\infty (1-\Theta)^{(1+\zeta)^2}\,\mathrm{d}\zeta.$$

In this calculation all of the islands have the same size whatever the value of Θ. It is a sort of mean field coalescence and, strictly speaking, is not exactly a kinetics ruled by coalescence, yet equation (74) works surprisingly well. As a matter of fact, we have performed many MC

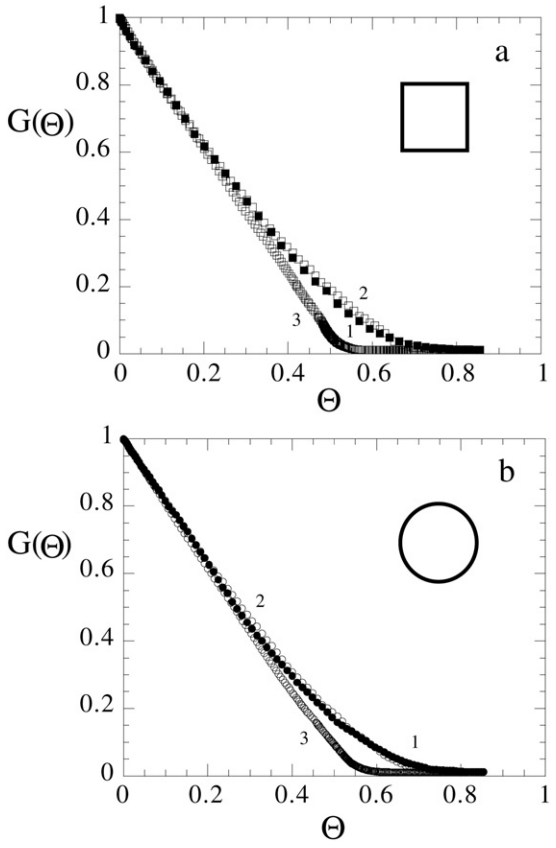

Figure 14. Comparison between the $G(\Theta)$ kinetics in the case of coalescence and impingement growth mechanisms and for simultaneous nucleation. The full symbols refer to the impingement case (curve 1) while open symbols refer to 2D (curve 2) and 3D (curve 3) island coalescence. (a) Square and cube. (b) Circle and hemisphere.

simulations both in the case of impingement and in the case of coalescence. In figure 14 we report one of the various computer outputs which shows that $G(\Theta)$ *does not change moving from coalescence to impingement* [12], and equation (74) is in very remarkable agreement with the numerical simulation as disclosed in figure 15 [51, 49]. In figure 16 we have reported also the comparison between the theoretical calculation (numerical simulation) and the experimental determination of $N(\Theta)$ obtained from the growth of diamond on an Si substrate [52]; the same specimen is described in section 3.1. This case can be considered paradigmatic for growth characterized by impingement. The good agreement between the data and the simulation corroborates, once more, the Poissonian character of this kind of growth, where, it is worth repeating, no diffusion of adspecies occurs.

The 'universal' scaling of the island density with respect to the growth mechanism already discussed has been recently exploited for analysing experimental data obtained from the growth of quaterthiophene films on silica substrate [53]. From the $N(\Theta)$ plot the authors were able to evaluate the nucleation density at saturation, that is achieved at the beginning of the deposition process (figure 17). It is worth noting that, in fact, such an analysis does not require atomic resolution microscopy techniques, for it is based on measurements carried out over the entire range of coverages.

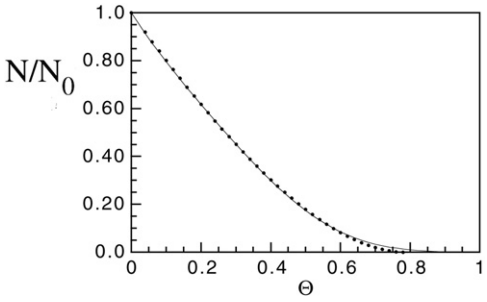

Figure 15. Island density versus surface coverage during simultaneous nucleation of thin film. Continuous line: analytical model of the 'mean field coalescence', equation (74). Dots: numerical solution in the case of square cluster growth ruled by the impingement mechanism.

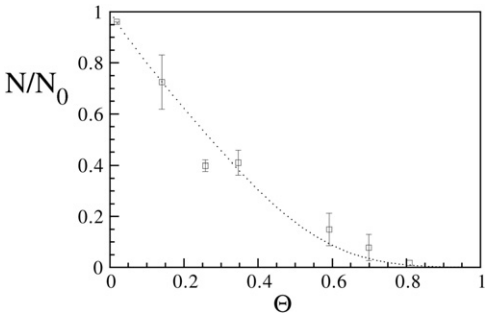

Figure 16. Experimental data on CVD growth of diamond film. The density of diamond islands, as a function of the surface coverage, is reported as open squares. In the same panel the kinetics of island aggregation as computed through equation (68) is also reported as dotted line.

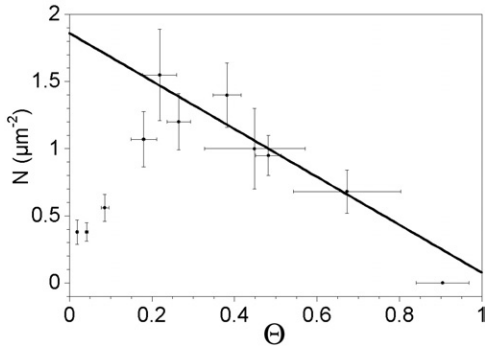

Figure 17. Behaviour of the island density as a function of fractional coverage, Θ, over the entire range of coverages ($0 < \Theta < 1$). Data refer to the growth of quaterthiophene thin films on silica substrate.

4. Rate equations

The processes that are taken into account in the traditional mean field rate equation (RE) approach [54] are the following: adsorption and desorption of monomers, diffusion of adatoms, nucleation, island growth and impingement/coalescence of islands. In the RE a critical size,

n^*, is assumed in such a way that nuclei with size larger than n^* can only grow by monomer addition. Detachment of monomers only involves sub-critical nuclei. The definition of a sharp critical size is necessary for the closure of the system of RE; as a matter of fact in this circumstance the system consists of $n^* + 1$ equations, one being the equation for the number density of stable nuclei: $n = \sum_{i>n*} n_i$. The system is not linear in the surface densities and, moreover, size dependent capture numbers σ_i, are defined representing the propensity of an island to capture the available adatoms [55, 56].

The simplest application of the RE method has been proposed by Logan in [57] for the case of stable dimers and total condensation of adatoms. By making use of dimensionless variables for the time as well as for the surface densities of both monomers and dimers, the numerical solution of the RE system is given in 'universal' form and can be employed for studying the nucleation stage for different parameter values. However, in this article, as well as in the majority of those dealing with RE, one studies only the early stage of film growth. To be specific, as already stated in section 3.3, the collision process of islands has rarely been treated, with the possible exception of [58] and [4], where the authors introduced a term which accounts approximatively for the island collision:

$$(\mathrm{d}N)_{\mathrm{coll}} = -2N\,\mathrm{d}\Theta. \tag{75}$$

This term can be used for describing just the initial stage of the collisional regime. In fact, to go further, up to $\Theta = 1$ it is necessary to employ equation (64) which, in the limit $\Theta \to 0$, coincides with equation (75). On the other hand, as far as the nucleation regime is concerned, remarkable results have been achieving in describing experimental [59] and computer simulation kinetics of the island density [13].

In the following we will dwell upon the issue of how to treat, over the whole coverage region, film growth governed by adatom diffusion. As a consequence, nuclei are not distributed at random throughout the substrate. The effect of this spatial correlation must be included in both the adatom lifetime and the collision series, but this is exactly what we have developed in the previous section.

We solve rate equations under the following assumptions: (i) total condensation of monomers, that is monomer evaporation does not occur; (ii) dimers are the stable nuclei; (iii) islands are two-dimensional; (iv) monomers landing on the islands contribute to the lateral growth of the film. Under these hypotheses the rate equations read

$$\begin{aligned} \frac{\mathrm{d}n_1}{\mathrm{d}t} &= F(1-\Theta) - \frac{n_1}{\tau} \\ \frac{\mathrm{d}n}{\mathrm{d}t} &= \frac{1}{2}G\frac{n_1}{\tau_{\mathrm{n}}} - \frac{n}{\tau_{\mathrm{c}}}, \end{aligned} \tag{76}$$

where F is the gas flux of monomers, n_1 is the number density of adatoms, n is the number of islands, τ_{c} is the characteristic time for island collision and $\tau^{-1} = \tau_{\mathrm{n}}^{-1} + \tau_{\mathrm{g}}^{-1}$, in which τ_{n} and τ_{g} are the characteristic times for nucleation and island growth respectively. The term G is the function introduced in section 3.3 (equation (64)). Equation (76) differs from the traditional equations in that the characteristic times are functions of time and in the presence of G. This deserves an explanation.

As evidenced in section 3.3 the function G takes into account the decay of the island number due to collision among islands in the case of simultaneous nucleation. How do we treat the case of non-simultaneous nucleation that is intrinsic to the rate equation scheme? A convenient way to answer this question is to employ the following approximation:

$$n(\Theta) = \nu(\Theta)G(\Theta), \tag{77}$$

where $\nu(\Theta)$ stands for the number of nucleation events that occurred up to Θ; i.e. for each coverage, the number of islands is given by the total number of nuclei (or clusters) weighted

by the collision function. This implies that, at each coverage, all the clusters have the same size. We have expressed the kinetics in terms of coverage, rather than time, because in this case G results as independent of the collisional mechanism i.e. impingement, coalescence or any intermediate case [12]. By taking the derivative of equation (77) we get

$$\begin{aligned}\frac{\mathrm{d}n}{\mathrm{d}t} &= \left(\frac{\mathrm{d}\nu}{\mathrm{d}t}G + \nu\frac{\mathrm{d}G}{\mathrm{d}\Theta}\dot{\Theta}\right)\\ &= \frac{\mathrm{d}\nu}{\mathrm{d}t}G + \nu G F\frac{\mathrm{d}\ln G}{\mathrm{d}\Theta}\\ &= \frac{\mathrm{d}\nu}{\mathrm{d}t}G - \frac{n}{\tau_{\mathrm{c}}},\end{aligned} \tag{78}$$

where the approximation $F \cong \dot{\Theta}$ has been used. This is an approximation since a fraction of the flux results in admonomers. Equation (78) discloses the important result

$$\frac{1}{\tau_{\mathrm{c}}(\Theta)} = -F\frac{\mathrm{d}\ln G(\Theta)}{\mathrm{d}\Theta}; \tag{79}$$

i.e. a function of surface coverage: $\Theta = Ft - n_1$. Equation (78) coincides with the second equation of equation (76). By writing the system in terms of coverage variable, we get

$$\begin{aligned}\frac{\mathrm{d}n_1}{\mathrm{d}\Theta} &= (1-\Theta) - \frac{n_1}{F\tau}\\ \frac{\mathrm{d}n}{\mathrm{d}\Theta} &= \frac{1}{2}G\frac{n_1}{F\tau_{\mathrm{n}}} - \frac{n}{F\tau_{\mathrm{c}}},\end{aligned} \tag{80}$$

where now the τs are functions of Θ. As far as the characteristic time of growth is concerned, it has been discussed in section 3.2. In particular, equation (57) must be used after having changed the variable t with Θ. As usual, the characteristic time for nucleation can be taken as

$$\frac{1}{\tau_{\mathrm{n}}(\Theta)} = 2\sigma_1 D n_1(1-\tilde{\Theta}), \tag{81}$$

σ_1 being the capture factor for the adatoms, D the diffusion coefficient and $\tilde{\Theta}$ the fraction of the substrate area in which nucleation is precluded because of the correlation among islands. In order to test this model, for want of experimental data, we used kinetic Monte Carlo (KMC) output from [60]. In figure 18 we show the $G(\Theta)$ obtained from equation (77) using $n(\Theta)$ and $\nu(\Theta)$ available from KMC output at $D/F = 10^5$. In the same figure also displayed are the fit of the KMC derived data and the numerical Monte Carlo (MC) simulation with $\Theta^* = 0.8$. The plots confirm what we have often underlined: that growth governed by adatom diffusion gives rise, naturally, to spatially correlated nuclei/islands. In this specific case, MC simulation of the $G(\Theta)$ kinetics is initially flat because of spatial correlation, which means that the clusters do not collide up to $\Theta_c = 0.2$. In fact, since $\Theta^* = Nl_{\mathrm{hc}}^2 = 0.8$ and because on average the first collision takes place at $l_{\mathrm{hc}} = 2l_c$, l_c being the cluster side, we get $\Theta_c = Nl_c^2 = \frac{\Theta^*}{4} = 0.2$. Moreover, the curve fit has been used in the numerical integration of the rate equations, which, as stated above, describes a non-simultaneous nucleation process.

In figure 19 we show the comparison between the island density behaviours obtained by KMC simulation and from rate equations [61]. In the same figure we also display the kinetics in the case of Poissonian distribution of islands and employing equation (75) instead of equation (64) to model the island collisions. As appears, the two main features of the kinetics are well reproduced by rate equations *only when the spatial correlation among nuclei is considered*: the maxima coincide and the tail correctly drops towards zero at large coverages.

Nevertheless, not only are rate equations successful for determining the island density behaviour in the presence of spatial correlation, as we showed already, but also they allow one

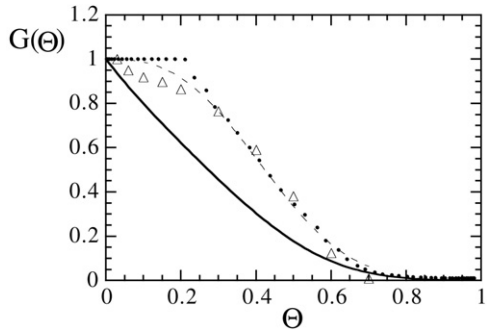

Figure 18. Collision series, $G(\Theta)$, for the simultaneous nucleation case. The full line and the dotted line represent, respectively, the random and spatially correlated distribution of nuclei. The Monte Carlo simulation of spatially correlated nuclei has been performed according to the hard core model at $S^* = 0.8$. The open symbols stand for the function obtained using the $n(\Theta)$ and $\nu(\Theta)$ functions available from the kinetic Monte Carlo simulation at $D/F = 10^5$ [60]. The dashed line is the best fit of a stretched exponential to the KMC curve.

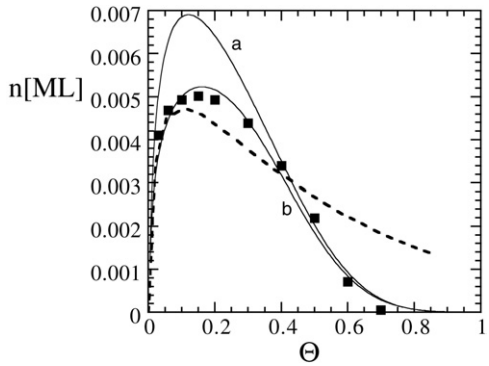

Figure 19. Number of islands, n, as a function of film thickness, Θ. The kinetics computed from rate equations at $D/F = 10^5$ and $p = 0.9$ (full lines) are compared to the KMC outputs of [60] (symbols), both for a random (curve a) and for a non-random (curve b) arrangement of nuclei. Rate equations have also been integrated using the time constant $\frac{1}{\tau_c} = 2F$. The result is displayed as a dashed line.

to model the island size distribution function. To this end it is compulsory to take into account correlation effects between the size of the island and the capture zone or VC (see also figure 1). This has been done, for instance, in [7] where a method is proposed that is based on classical mean field rate equations [54]. The core of the model is the evaluation of capture numbers. In particular, rate equations have been formulated which give the evolution of the Voronoi cell distribution of islands of size s: $f_s(A, \Theta)$, A being the area of the capture zone. Thanks to a mean field approximation the solution for the joint probability distribution $f_s(A, \Theta)$ has been computed analytically. Furthermore, on the basis of the Bales and Chrzan approach [13] the local capture numbers, $\tilde{\sigma}_s(A)$, are also determined and with them the average capture numbers, $\sigma_s = \langle \tilde{\sigma}_s(A) \rangle_{f_s(A)}$, that enter in their rate equation scheme. It is shown that by using the σ_s s the integration of rate equations leads to an excellent description of Monte Carlo results for both island size and capture number distributions.

Interestingly for suitable choices of the rate coefficients, rate equations can also be employed for dealing with correlation between island size and local environment. The model

presented in [7] does not include the break-up of Voronoi cells when new islands are nucleated. The latter process as well as the scaling properties of the joint probability distribution have been thoroughly treated in [62].

It has to be noted that the papers dealing with the local environment correlation are confined to the investigation of the pre-coalescence regime where collisions among islands can be, just by reason of the nucleation forbidden zone, safely neglected, each island being associated with a single nucleation event. In other words, while those approaches resolve in detail the early stage regime (up to $\Theta \lesssim 0.2$), the model reviewed here has been elaborated for describing the kinetics up to the film closure. Clearly the analytical resolution of the rather demanding latter requirement calls for approximations. For example, at odds with the approach of [7], our model makes use of an average island capture number which depends, however, upon surface coverage [45]:

$$\sigma(\Theta) = \frac{1}{\tau'(\Theta)G(\Theta)};$$

it is a combination of both adatom lifetime and collision series.

At the very end, a last citation is in order. It has been shown that the solutions of rate equations in the pre-coalescence regime also exhibit scaling properties with respect to the deposition and materials parameters. This has been shown analytically in [63] for the behaviour of the island size distribution function and adatom density. The validity of the scaling hypothesis in the case of reversible aggregation has been discussed in [64] on the basis of MC simulations.

5. Conclusions

In this article we have reviewed some aspects related to the modelling of thin film growth kinetics through stochastic processes of dots. The approach presented here is based on the integration of rate equations which, very often, have been used in the low coverage regime and for random distribution of nuclei. To extend this approach to the full range of coverage and to the case of spatially correlated nuclei, it is compulsory to elaborate a model for the characteristic times, such that it could be easily used in a rate equation scheme. The key point is that, by exploiting the growth law of the average cluster, the main ingredients of rate equations are two quantities: $G(\Theta; \Theta^*)$ and $\tau(\Theta; \Theta^*)$. The computation can be worked out, analytically, on the basis of a stochastic approach in which the fundamental role is played by the exclusion probability.

Acknowledgment

One of the authors (MF) dedicates this work to his grandparent, Delma e Alfredo, recently passed away.

Appendix A

The mean value of N, as defined in equation (2), can be evaluated as follows:

$$\begin{aligned}\langle N\rangle &= \sum_{s=1}^{\infty}\frac{1}{s!}\int \mathrm{d}\mathbf{x}^s N_s(\mathbf{x}_1,\ldots,\mathbf{x}_s)\,Q_s(\mathbf{x}_1,\ldots,\mathbf{x}_s)\\ &= \sum_{s=1}^{\infty}\frac{1}{s!}\int \mathrm{d}\mathbf{x}^s \sum_{k=1}^{s}\chi(\mathbf{x}_k)\,Q_s(\mathbf{x}_1,\ldots,\mathbf{x}_s)\end{aligned}$$

$$= \sum_{s=1}^{\infty} \frac{1}{s!} \sum_{k=1}^{s} \int_{\Delta} \mathrm{d}\mathbf{x}_k \int \mathrm{d}\mathbf{x}^{s-1} Q_s(\mathbf{x}_1, \ldots, \mathbf{x}_s)$$

$$= \sum_{s=1}^{\infty} \frac{1}{(s-1)!} \int_{\Delta} \mathrm{d}\mathbf{x}_1 \int \mathrm{d}\mathbf{x}^{s-1} Q_s(\mathbf{x}_1, \ldots, \mathbf{x}_s), \tag{83}$$

where in shorthand notation $\mathrm{d}\mathbf{x}^s \equiv \mathrm{d}\mathbf{x}_1\, \mathrm{d}\mathbf{x}_2 \ldots \mathrm{d}\mathbf{x}_s$ and the last step exploits the symmetry of the Q_s s. By the same token it is possible to show that

$$\left\langle N^2 \right\rangle = \langle N \rangle + \sum_{s=2}^{\infty} \frac{1}{(s-2)!} \int_{\Delta} \mathrm{d}\mathbf{x}_1 \int_{\Delta} \mathrm{d}\mathbf{x}_2 \int \mathrm{d}\mathbf{x}^{s-2}\, Q_s(\mathbf{x}_1, \ldots \mathbf{x}_s). \tag{84}$$

On the basis of (83) and (84) the following functions can be introduced:

$$f_1(\mathbf{y}_1) = \sum_{s=1}^{\infty} \frac{1}{(s-1)!} \int \mathrm{d}\mathbf{x}^{s-1}\, Q_s(\mathbf{y}_1, \mathbf{x}_2, \ldots, \mathbf{x}_s)$$

$$f_2(\mathbf{y}_1, \mathbf{y}_2) = \sum_{s=2}^{\infty} \frac{1}{(s-2)!} \int \mathrm{d}\mathbf{x}^{s-2}\, Q_s(\mathbf{y}_1, \mathbf{y}_2, \mathbf{x}_3, \ldots, \mathbf{x}_s)$$

$$\ldots\ldots\ldots\ldots\ldots\ldots\ldots$$

$$f_n(\mathbf{y}_1, \ldots, \mathbf{y}_n) = \sum_{s=n}^{\infty} \frac{1}{(s-n)!} \int \mathrm{d}\mathbf{x}^{s-n}\, Q_s(\mathbf{y}_1, \mathbf{y}_2, \ldots, \mathbf{y}_n, \mathbf{x}_{n+1} \ldots, \mathbf{x}_s), \tag{85}$$

which allow one to rewrite (83) and (84) as (3) and (4).

Appendix B

The mean values of the generic function V defined in equation (6) are quickly evaluated as follows:

$$\begin{aligned}
\langle V \rangle &= \sum_{s=1}^{\infty} \frac{1}{s!} \int \mathrm{d}\mathbf{x}^s\, Q_s(\mathbf{x}_1, \ldots, \mathbf{x}_s) \sum_{k=1}^{s} v(\mathbf{x}_k) \\
&= \sum_{s=1}^{\infty} \frac{1}{(s-1)!} \int \mathrm{d}\mathbf{x}^s\, Q_s(\mathbf{x}_1, \ldots, \mathbf{x}_s) v(\mathbf{x}_1) \\
&= \int \mathrm{d}\mathbf{x}_1\, v(\mathbf{x}_1) f_1(\mathbf{x}_1)
\end{aligned}$$

$$\begin{aligned}
\left\langle V^2 \right\rangle &= \sum_{s=1}^{\infty} \frac{1}{s!} \int \mathrm{d}\mathbf{x}^s\, Q_s(\mathbf{x}_1, \ldots, \mathbf{x}_s) \sum_{\nu=1}^{s} v(\mathbf{x}_\nu) \sum_{\mu=1}^{s} v(\mathbf{x}_\mu) \\
&= \sum_{s=1}^{\infty} \frac{1}{s!} \int \mathrm{d}\mathbf{x}^s\, Q_s \left[\sum_{\mu=1}^{s} v^2(\mathbf{x}_\mu) + 2 \sum_{\mu<\nu}^{s} v(\mathbf{x}_\mu) v(\mathbf{x}_\nu) \right] \\
&= \sum_{s=1}^{\infty} \frac{1}{(s-1)!} \int \mathrm{d}\mathbf{x}^s\, Q_s v(\mathbf{x}_1) + \sum_{s=2}^{\infty} \frac{1}{(s-2)!} \int \mathrm{d}\mathbf{x}^s\, Q_s v(\mathbf{x}_1) v(\mathbf{x}_2) \\
&= \int \mathrm{d}\mathbf{x}_1\, v^2(\mathbf{x}_1) f_1(\mathbf{x}_1) + \int \mathrm{d}\mathbf{x}_1\, \mathrm{d}\mathbf{x}_2\, v(\mathbf{x}_1) v(\mathbf{x}_2) f_2(\mathbf{x}_1, \mathbf{x}_2).
\end{aligned} \tag{86}$$

Appendix C

The average of $V^{(1)}$ reads

$$\begin{aligned}\left\langle V^{(1)}\right\rangle_{\{1\}} &= \sum_{\{1\}}\sum_{s}\sum_{\Pi^s_{\{1\}}}\frac{1}{n_i!}\int Q^{(1)}_{\pi^s_i}\sum_{\langle 1\rangle} v_i\,\mathrm{d}\mathbf{x}^s \\ &= \sum_{\{1\}}\sum_{s}\sum_{\Pi^s_{\{1\}}}\frac{1}{(n_i-1)!}\int v_i\,\mathrm{d}\mathbf{x}_i\int Q^{(1)}_{\pi^s_i}\,\mathrm{d}\mathbf{x}^{s-1} \\ &= \sum_{\{1\}}\int v_i h_i\,\mathrm{d}\mathbf{x}_1 = \sum_{\{1\}}(v_i h_i),\end{aligned} \tag{87}$$

where we have introduced the function

$$h_i(\mathbf{x}_1) \equiv \sum_{s}\sum_{\Pi^s_{\{1\}}}\frac{1}{(n_i-1)!}\int Q^{(1)}_{\pi^s_i}\,\mathrm{d}\mathbf{x}^{s-1}. \tag{88}$$

Similarly we obtain

$$\left\langle V^{(2)}\right\rangle_{\{2\}} = \sum_{\{1\}}\sum_{\{1\}\backslash i}(v_i h_{i,j}) \tag{89}$$

$$\left\langle V^{(3)}\right\rangle_{\{3\}} = \sum_{\{1\}}\sum_{\{2\}\backslash i}(v_i h_{i,jk}), \tag{90}$$

where

$$h_{i,j}(\mathbf{x}_1) \equiv \sum_{s}\sum_{\Pi^s_{\{2\}}}\frac{1}{(n_i-1)!n_j!}\int Q^{(2)}_{\pi^s_{ij}}\,\mathrm{d}\mathbf{x}_i^{n_i-1}\,\mathrm{d}\mathbf{x}_j^{n_j}, \tag{91}$$

$$h_{i,jk}(\mathbf{x}_1) \equiv \sum_{s}\sum_{\Pi^s_{\{3\}}}\frac{1}{(n_i-1)!n_j!n_k!}\int Q^{(3)}_{\pi^s_{ijk}}\,\mathrm{d}\mathbf{x}_i^{n_i-1}\,\mathrm{d}\mathbf{x}_j^{n_j}\,\mathrm{d}\mathbf{x}_k^{n_k} \tag{92}$$

and the symbol $\{m\}\backslash i$ means that all the m-tuples are considered that do not contain the i-class. In addition, the f-function of any specific class can be defined as

$$f_i \equiv h_i + \sum_{\{1\}\backslash i} h_{i,j} + \sum_{\{2\}\backslash i} h_{i,jk} + \sum_{\{3\}\backslash i} h_{i,jkl} + \cdots \tag{93}$$

and

$$f_{ij} \equiv h_{ij} + \sum_{\{1\}\backslash i,j} h_{ij,k} + \cdots \tag{94}$$

where

$$h_{ij,k} \equiv \sum_{s}\sum_{\Pi^s_{\{3\}}}\frac{1}{(n_i-1)!(n_j-1)!n_k!}\int Q^{(3)}_{\pi^s_{ijk}}\,\mathrm{d}\mathbf{x}_i^{n_i-1}\,\mathrm{d}\mathbf{x}_j^{n_j-1}\,\mathrm{d}\mathbf{x}_k^{n_k}. \tag{95}$$

Appendix D

We will show the equivalence between equations (30) and (31) just for the case $s = 3$; for the others the reader can proceed in a like manner. From equation (30) it follows that

$$A = \sum_{m}\sum_{\{m\}}\sum_{\Pi^s_{\{m\}}}\frac{\int_{\Delta_1}\mathrm{d}\mathbf{x}_1^{n_1^3}\ldots\int_{\Delta_m}\mathrm{d}\mathbf{x}_m^{n_m^3}\,g_3}{n_1!\ldots n_m!}$$

$$
\begin{aligned}
&= \sum_{\{1\}} \sum_{\Pi^3_{\{1\}}} \frac{1}{n_1!} \int_{\Delta_1} \mathrm{d}\mathbf{x}_1^{n_1^3} g_3 + \sum_{\{2\}} \sum_{\Pi^3_{\{2\}}} \frac{1}{n_1! n_2!} \int_{\Delta_1} \mathrm{d}\mathbf{x}_1^{n_1^3} \int_{\Delta_2} \mathrm{d}\mathbf{x}_2^{n_2^3} g_3 \\
&\quad + \sum_{\{3\}} \sum_{\Pi^3_{\{3\}}} \frac{1}{n_1! n_2! n_3!} \int_{\Delta_1} \mathrm{d}\mathbf{x}_1^{n_1^3} \int_{\Delta_2} \mathrm{d}\mathbf{x}_2^{n_2^3} \int_{\Delta_3} \mathrm{d}\mathbf{x}_3^{n_3^3} g_3 \\
&= \sum_{\{1\}} \frac{1}{3!} \int_{\Delta_i} \mathrm{d}\mathbf{x}_1^{(i)} \mathrm{d}\mathbf{x}_2^{(i)} \mathrm{d}\mathbf{x}_3^{(i)} g_3(\mathbf{x}_1^{(i)}, \mathbf{x}_2^{(i)}, \mathbf{x}_3^{(i)}) \\
&\quad + \sum_{\{2\}} \frac{1}{2!1!} \int_{\Delta_i} \mathrm{d}\mathbf{x}_1^{(i)} \mathrm{d}\mathbf{x}_2^{(i)} \int_{\Delta_j} \mathrm{d}\mathbf{x}_1^{(j)} g_3(\mathbf{x}_1^{(i)}, \mathbf{x}_2^{(i)}, \mathbf{x}_1^{(j)}) \\
&\quad + \sum_{\{2\}} \frac{1}{1!2!} \int_{\Delta_i} \mathrm{d}\mathbf{x}_1^{(i)} \int_{\Delta_j} \mathrm{d}\mathbf{x}_1^{(j)} \mathrm{d}\mathbf{x}_2^{(j)} g_3(\mathbf{x}_1^{(i)}, \mathbf{x}_1^{(j)}, \mathbf{x}_2^{(j)}) \\
&\quad + \sum_{\{3\}} \frac{1}{1!1!1!} \int_{\Delta_i} \mathrm{d}\mathbf{x}_1^{(i)} \int_{\Delta_j} \mathrm{d}\mathbf{x}_1^{(j)} \int_{\Delta_k} \mathrm{d}\mathbf{x}_1^{(k)} g_3(\mathbf{x}_1^{(i)}, \mathbf{x}_1^{(j)}, \mathbf{x}_1^{(k)}),
\end{aligned}
$$

and from equation (31)

$$
\begin{aligned}
B &= \frac{1}{3!} \sum_i \sum_j \sum_k \rho_i \rho_j \rho_k \int_{\Delta_i} \mathrm{d}\mathbf{x}_1^{(i)} \int_{\Delta_j} \mathrm{d}\mathbf{x}_1^{(j)} \int_{\Delta_k} \mathrm{d}\mathbf{x}_1^{(k)} \tilde{g}_3 \\
&= \frac{1}{3!} \Bigg[\sum_{\{1\}} \rho_i^3 \int_{\Delta_i} \mathrm{d}\mathbf{x}_1^{(i)} \mathrm{d}\mathbf{x}_2^{(i)} \mathrm{d}\mathbf{x}_3^{(i)} \tilde{g}_3(\mathbf{x}_1^{(i)}, \mathbf{x}_2^{(i)}, \mathbf{x}_3^{(i)}) \\
&\quad + 3 \sum_{\{2\}} \rho_i^2 \rho_j \int_{\Delta_i} \mathrm{d}\mathbf{x}_1^{(i)} \mathrm{d}\mathbf{x}_2^{(i)} \int_{\Delta_j} \mathrm{d}\mathbf{x}_1^{(j)} \tilde{g}_3(\mathbf{x}_1^{(i)}, \mathbf{x}_2^{(i)}, \mathbf{x}_1^{(j)}) \\
&\quad + 3 \sum_{\{2\}} \rho_i \rho_j^2 \int_{\Delta_i} \mathrm{d}\mathbf{x}_1^{(i)} \int_{\Delta_j} \mathrm{d}\mathbf{x}_1^{(j)} \mathrm{d}\mathbf{x}_2^{(j)} \tilde{g}_3(\mathbf{x}_1^{(i)}, \mathbf{x}_1^{(j)}, \mathbf{x}_2^{(j)}) \\
&\quad + \sum_{\{3\}} \rho_i \rho_j \rho_k \int_{\Delta_i} \mathrm{d}\mathbf{x}_1^{(i)} \int_{\Delta_j} \mathrm{d}\mathbf{x}_1^{(j)} \int_{\Delta_k} \mathrm{d}\mathbf{x}_1^{(k)} \tilde{g}_3(\mathbf{x}_1^{(i)}, \mathbf{x}_1^{(j)}, \mathbf{x}_1^{(k)}) \Bigg].
\end{aligned}
$$

So, because of equation (32), we get

$$A = B. \tag{96}$$

References

[1] King D A and Woodruff D P (ed) 1997 *Growth and Properties of Ultra Thin Epitaxial Layer in The Chemical Physics of Solid Surfaces* vol 8 (Amsterdam: Elsevier)
[2] Budevski E, Staikov G and Lorenz W J 1996 *Electrochemical Phase Formation and Growth* (New York: VCH)
[3] Aicha E-R and Barlow F D 1997 *Thin Film Technology Handbook* (New York: McGraw-Hill)
[4] Venables J A 1973 *Phil. Mag.* **17** 697
[5] Mulheran P A and Blackman J A 1995 *Phil. Mag. Lett.* **72** 55
Mulheran P A and Blackman J A 1996 *Phys. Rev.* B **53** 10261
[6] Okabe A, Boots B, Sugihara K and Chin S N 2000 *Spatial Tessellations. Concept and Application of Voronoi Diagrams* 2nd edn (New York: Wiley)
[7] Amar J G, Popescu M N and Family F 2001 *Phys. Rev. Lett.* **86** 3092
[8] Bartelt M C, Stoldt C R, Jenks C J, Thiel P A and Evans J W 1999 *Phys. Rev.* B **59** 3125
[9] Ngo T T, Petroff P M, Sakaki H and Merz J L 1996 *Phys. Rev.* B **53** 9618
[10] Yang Y-N, Luo Y S and Weaver J H 1992 *Phys. Rev.* B **46** 15387
[11] Cherepanov V, Filimonov S, Mysliveček J and Voigtländer B 2004 *Phys. Rev.* B **70** 085401
[12] Fanfoni M, Tomellini M and Volpe M 2001 *Phys. Rev.* B **64** 075409

[13] Bales G S and Chrzan D C 1994 *Phys. Rev.* B **50** 6057
[14] Barabási A-L and Stanley H E 1995 *Fractal Concept in Surface Growth* (Cambridge: Cambridge University Press)
[15] Brune H 1998 *Surf. Sci. Rep.* **31** 121
[16] Tomellini M and Fanfoni M 2001 *Curr. Opin. Solid State Mater. Sci.* **5** 91
[17] Van Kampen N G 1992 *Stochastic Processes in Physics and Chemistry* (Amsterdam: North-Holland)
[18] Fanfoni M and Tomellini M 2003 *Eur. Phys. J.* B **34** 331
[19] Tomellini M, Fanfoni M and Volpe M 2002 *Phys. Rev.* B **65** 140301(R)
[20] Fanfoni M and Tomellini M 1998 *Nuovo Cimento* **20** 1171
[21] Birnie D P III and Weinberg M C 1995 *J. Chem. Phys.* **91** 3742
[22] Kolmogorov A N 1937 *Bull. Acad. Sci. URSS (cl. Sci. Math. Nat.)* **3** 355
[23] Johnson W A and Mehl R F 1939 *Trans. Am. Inst. Min., Metall. Pet. Eng.* **135** 416
[24] Avrami M 1939 *J. Chem. Phys.* **7** 1103
Avrami M 1940 *J. Chem. Phys.* **8** 212
[25] Tomellini M and Fanfoni M 1997 *Phys. Rev.* B **55** 14071
[26] Tomellini M and Fanfoni M 2004 *Physica* A **333** 65
[27] Holloway P H and Hudson J B 1974 *Surf. Sci.* **43** 123
[28] Behm R J, Ertl G and Wintterlin J 1986 *Ber. Bunsenges. Phys. Chem.* **90** 294
[29] Polini R, Tomellini M, Fanfoni M and Le Normande F 1997 *Surf. Sci.* **373** 230
[30] Tomellini M and Fanfoni M 1996 *Surf. Sci.* **349** L191
[31] Chiew Y C and Glandt E D 1984 *J. Colliod Interface Sci.* **99** 86
[32] Trofimov V I and Park H S 2003 *Appl. Surf. Sci.* **219** 93
[33] Trofimov V I 2000 *Thin Solid Films* **380** 64
[34] Hermann H, Mattern N, Roth S and Uebele P 1997 *Phys. Rev.* B **56** 13888
[35] Tomellini M, Fanfoni M and Volpe M 2000 *Phys. Rev.* B **62** 11300
[36] Tong W S, Rickman J M and Barmak K 2001 *J. Chem. Phys.* **114** 915
[37] Hansen J P and McDonald I R 1986 *Theory of Simple Liquids* 2nd edn (London: Academic)
[38] Tobin M C 1974 *J. Polym. Sci., Polym. Chem. Edn.* **12** 399
[39] Schaaf P and Talbot J 1989 *Phys. Rev. Lett.* **62** 175
[40] Torquato S and Stell G 1984 *J. Chem. Phys.* **80** 878
[41] Reiss H, Frisch H L and Lebowitz J L 1939 *J. Chem. Phys.* **31** 369
[42] Tagami T and Tanaka S-I 1997 *Acta Mater.* **45** 3341
[43] Dickman R, Wang J-S and Jensen I 1991 *J. Chem. Phys.* **94** 8252
[44] Fanfoni M, Tomellini M and Volpe M 2002 *Phys. Rev.* B **65** 172301
[45] Tomellini M and Fanfoni M 1999 *Surf. Sci.* **440** L849
[46] Hughes B D 1995 *Random Walks and Random Environments* (Oxford: Oxford Science Publications)
[47] Fanfoni M and Tomellini M 2004 *Surf. Sci.* **566–568** 1147
[48] Fanfoni M and Tomellini M 1998 *Appl. Surf. Sci.* **136** 338
[49] Volpe M, Fanfoni M, Tomellini M and Sessa V 1999 *Surf. Sci. Lett.* **440** L820
[50] Briscoe B J and Galvin K P 1991 *Phys. Rev.* A **43** 1906
[51] Tomellini M and Fanfoni M 2000 *Surf. Sci.* **450** L267
[52] Fanfoni M, Polini R, Sessa V, Tomellini M and Volpe M 1999 *Appl. Surf. Sci.* **152** 126
[53] Campione M, Borghese A, Moret M and Sassella A 2003 *J. Mater. Chem.* **13** 1669
[54] Zinsmeister G 1968 *Thin Solid Films* **2** 497
Zinsmeister G 1969 *Thin Solid Films* **4** 363
Zinsmeister G 1971 *Thin Solid Films* **7** 51
[55] Gibou F, Ratsch C and Caflisch R 2003 *Phys. Rev.* B **67** 155403
[56] Venables J A and Brune H 2002 *Phys. Rev.* B **66** 195404
[57] Logan R M 1969 *Thin Solid Films* **3** 59
[58] Stowell M J and Hutchinson T E 1971 *Thin Solid Films* **8** 41
[59] Brune H, Röder H, Boragno C and Kern K 1994 *Phys. Rev. Lett.* **73** 1955
[60] Brune H, Bales G S, Jacobsen J, Boragno C and Kern K 1999 *Phys. Rev.* B **60** 5991
[61] Fanfoni M, Tomellini M and Volpe M 2001 *Appl. Phys. Lett.* **78** 3424
[62] Evans J W and Bartelt M C 2002 *Phys. Rev.* B **66** 235410
[63] Blackman J A and Wilding A 1991 *Europhys. Lett.* **16** 115
[64] Dobbs H T, Vvedensky D D, Zangwill A, Johansson J, Carlsson N and Seifert W 1997 *Phys. Rev. Lett.* **79** 897